2015-01-01

Aerosol Physical and Chemical Properties over Tropical Atlantic Ocean

Elsa Castillo
University of Texas at El Paso, ecastillo5@miners.utep.edu

AEROSOL PHYSICAL AND CHEMICAL PROPERTIES OVER THE TROPICAL ATLANTIC OCEAN

ELSA CASTILLO

DOCTORAL PROGRAM IN ENVIRONMENTAL SCIENCE AND ENGINEERING

APPROVED:

_____
Rosa Fitzgerald, Ph.D., Chair

_____
Vernon Morris, Ph.D., Co-Chair

_____
Barry Benedict, Ph.D.

_____
Sergio Flores, Ph.D.

_____
Charles H. Ambler, Ph.D.
Dean of the Graduate School

AEROSOL PHYSICAL AND CHEMICAL PROPERTIES OVER THE TROPICAL ATLANTIC OCEAN

by

ELSA CASTILLO, M.Sc.

Presented to the Faculty of the Graduate School of

The University of Texas at El Paso

in Partial Fulfillment

of the Requirements

for the Degree of

DOCTOR OF PHILOSOPHY

ENVIRONMENTAL SCIENCE AND ENGINEERING

THE UNIVERSITY OF TEXAS AT EL PASO

MAY 2015

Acknowledgements

I would like to express my gratitude to Drs. Vivian Incera and Efrain Ferrer, who encouraged me to pursue a master's degree in physics and a Ph.D. in environmental science and engineering at the University of Texas El Paso (UTEP). I thank Dr. Rosa Fitzgerald for accepting me in her research group and Dr. Vernon Morris for giving me the opportunity to participate in three expeditions over the tropical Atlantic Ocean. I also thank my committee members, Drs. Sergio Flores and Barry Benedict for accepting being part in the development of my dissertation.

I thank Claudia Rodriguez, Gloria Espinoza, Gloria Sapiens, Natalia Savchenko, Rosette Gonzalez, and Ebony Roper, my friends and family here in United States. I thank my family in Cuba for they continued support and praise and Federico Gutt (mi Lindo) for his patience, understanding, and love. Thank you to all people that I do not mention by name, but they have made possible this dissertation.

The Office of Education, Educational Partnership Program award, which is administered by the National Oceanic and Atmospheric Administration (NOAA)

made this work possible. Its contents are solely the responsibility of the award recipient and do not necessarily represent the official views of the U.S. Department of Commerce, National Oceanic and Atmospheric Administration.

Abstract

The atmospheric aerosol mass size distributions, modal characteristics, and a comparative analysis of the characteristic of $PM_{2.5}$ versus trace gases: CO, O_3, and SO_2 over tropical Atlantic Ocean have been evaluated for Nov-Dec 2013. This study took place during the IX AEROSE expedition while the National Oceanic and Atmospheric Administration (NOAA) research vessel Ronald H. Brown traveled south along 23°W between 3°N and 5°S.

Aerosol mass size distributions were measured directly with a California Instruments Model PC-2H Quartz Crystal Microbalance (QCM). The corresponding values of average mass for accumulation, nuclei and coarse mode obtained were: 0.00124±0.00077, 0.00506±0.00254, and 0.00176±0.00114 μg/m³. Mass median aerodynamic diameter (MMAD) ranged from 0.57 to 0.72 μm and geometric standard deviation between 1.62 and 2.18 for accumulation mode, were calculated.

The presence of CO, SO_2, O_3 (trace gases), and $PM_{2.5}$ that are well known as atmospheric pollutants was analyzed over the marine boundary layer of the tropical Atlantic Ocean. For Dec 1-4 the obtained mean aerosol mass

concentrations were: 29320±7953 μg/m³ for CO, 4.52±1.04 μg/m³ for SO_2, 792±190 μg/m³ for O_3, and 0.582±0.12 μg/m³ for $PM_{2.5}$.

The significance of the measurements obtained is emphasized in light of the comparative scarcity of such data over the tropical Atlantic Ocean.

Table of Contents

List of Tables

List of Figures

1. Introduction

"What connects Earth's largest, hottest desert to its largest tropical rain forest?" (NASA's Goddard Space Flight Center, 2015) Dust, and not a small quantity, between 60 and 200 million tons of dust per year connect Saharan dessert and the Amazonia (Lau, 2007). How many monitoring stations exist over the tropical Atlantic Ocean? None. The importance of this work is because the Saharan dust has a deep impact on global climatology, ecosystem, and human health, yet available data is scarce over the tropical Atlantic Ocean.

It is imperative to characterize the aerosol properties since they play a dominant role in the earth atmosphere energy balance system. Being able to quantify the aerosol contribution on weather and climate processes will result in a great step to improve our understanding and predict capabilities of aerosol processes, and their downstream effects on human and environmental health (Twomey S. , 1977); (Charlson, 1992); (IPCC 2007).

Aerosols are liquid and solid particles suspended in a gas, and can be seen in the smoke of a volcanic eruption as well as a forest fire, they could also be found in an

incomplete combustion of fossil fuels, as well as in traffic-related suspensions of roads. Aerosols can be flown in the air as plant fragments, microorganisms, or pollen, as well as in a hazy horizon (Reist, 1984).

Atmospheric aerosols have a significant impact on weather, climate, the environment, and human health. Several studies have demonstrated the crucial role of aerosols in global energy balance and emphasized the fact that aerosol particles, in contrast to greenhouse gases, can act in both directions: scattering solar radiation and cooling the Earth; absorbing solar radiation and warming the Earth (Intergovernmental Panel on climate change, 2007).

The Earth's surface is the main source for producing aerosols. Through a mechanical disintegration process, small particles are detached, elevated, and transported by the wind. The smaller and lighter ones travel longer distances, however the bigger ones are deposited in a short time due to their heavier masses (Gillette, 1977).

The soil particle diameter varies between 0.2 to 100 μm (Duce, 1985) and depend on the physical characteristics of the soil like water content, and the presence of vegetation together with specific meteorological conditions like wind speed (Ginoux, 2001). It is known that soil aerosols are characterized by a size mode

larger than those particles originated by human activities; consequently they have a greater role as radiative forcing (Haywood, 2005).

Because of adhesion and aggregation properties of fine particles, it is unusual that particles size <0.1 μm will be released to the atmosphere (Scheffer, 1992). However, soil particles >10 μm are too heavy to be transported long distances. Thus the typical mineral dust size is found between 0.1-10 μm (Todd, 2008).

Atmospheric soil dust has a large spatial and temporal variability. Some experts consider that aridity is a sign for dust source (Jennings, 1991), however others (Prospero J. M., 2002) consider that aridity by itself is not enough to identify the dust sources since Australia has an extent desert area, but a low dust release. It is considered that almost 50% worldwide atmospheric dust load is a product of land conversion: agriculture, urbanization, and logging (Tegen, 1996).

Africa is home to the world's largest non-polar desert, and a source of mineral dust, the Saharan Desert, which covers an area of more than 8 million square kilometers and injects the African firmaments with dust (Estupinan, 2012) as it is illustrated in Figure 1.

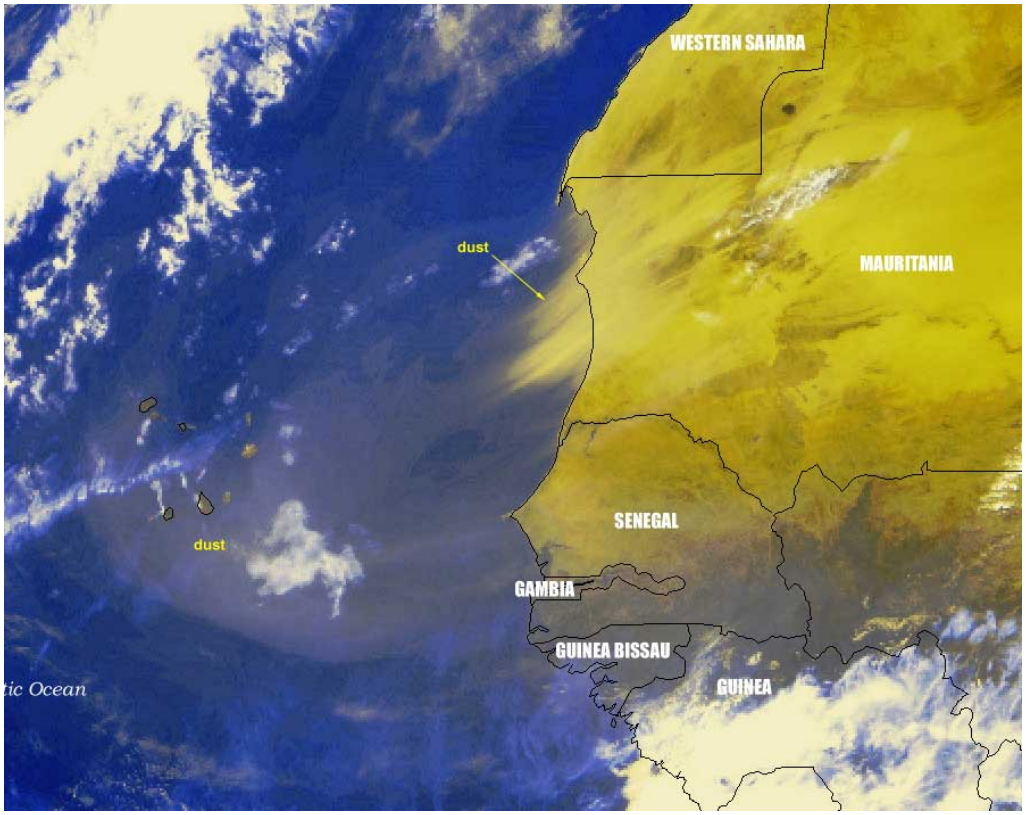

Figure 1. Dust storms exiting northwest Africa (Satellite-dust-6-16-1999.jpg, 1999)

The tropical Atlantic Ocean witnesses the mineral dust transport from the West-African coast to the Caribbean Sea for a full week (Huang, 2010)(Figure 2).

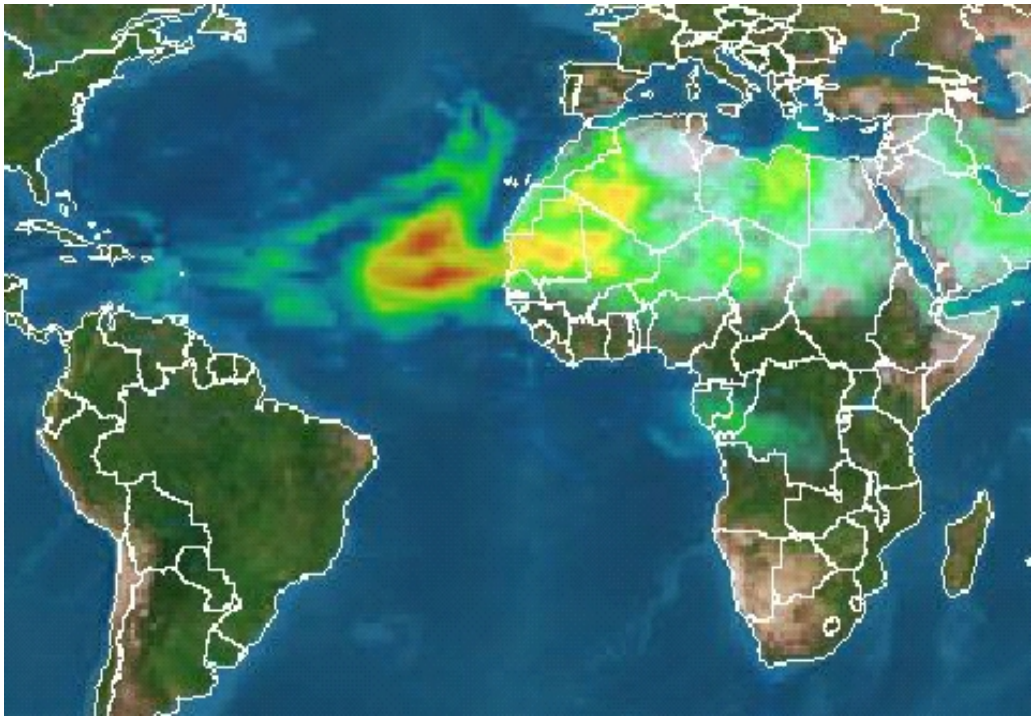

Figure 2. Saharan dusts moving across the Atlantic (TOMS dust and smoke (equatorial Africa), 1999)

In general, dust storms are a serious problem for humans and environmental health because they affect the air quality regionally and globally (Reid, 1994), (Prospero J. , 1979).

Since the general principles that govern the aerosol behavior are still an enigma, it is necessary to continue investigating their behavior over the ocean and land, as well as their impact on weather and climate processes. Our lack of understanding

about atmospheric aerosols is due to the ambiguity and inconsistencies in particle size distribution assessment (Reddy, 2012).

The determination of aerosol mass composition as a function of size can help determine the origin, the formation mechanism and atmospheric behavior of aerosols. Such knowledge is fundamental for data assimilation and to improve aerosol prediction models (Nair, 2008).

A large number of scientific expeditions have been conducted over the world's distinct oceans. The data collected during these ocean missions have substantially enriched our knowledge about the variability of aerosol physical and chemical properties in those regions (Smirnov, 1995); (Sakerin, 2002); (Moorthy, 2005).

The AERosol Ocean Science Expeditions (AEROSE) are a series of trans-Atlantic research cruises conducted onboard the National Oceanic and Atmospheric Administration (NOAA) research vessel Ronald H. Brown. The one of AEROSE's goals is to characterize the microphysical evolution and effect of African dust and smoke aerosol outflows across the Atlantic Ocean (Morris, 2006) (Nalli N. , 2011) (Atia, 2010).

2. Hourly Size Distribution of Aerosol Mass Concentration over the Tropical Atlantic Ocean (Observed During Saharan Dust Episodes)

Aerosols pose a serious threat to both human and environmental health because they affect the air quality regionally and globally (Reid, 1994; Prospero, 2002). In addition disturb the global climatology by changing the radiation budget directly by scattering the solar radiation, and indirectly by changing the physical properties of clouds (Roberts, 2009).

The atmosphere over the tropical Atlantic Ocean is disturbed by both Saharan dust and African biomass burning emissions (Roberts, 2009), (Huang, 2010). Africa is home to the world's largest non-polar desert, the Sahara desert, which covers an area of more than eight million square kilometers. The Sahara desert is a source of mineral dust, which gets injected into the African sky as indicated by Estupinan (Estupinan, 2012). The African continent is the major source of biomass burning releases (Roberts, 2009). Activities such as bush fires, forest fires, and wood-fuel are the three main sources of biomass burnings, which have a great impact on the tropical chemistry of the atmosphere. The transport of mineral dust over the Atlantic Ocean from the West African coast to the Caribbean Sea

takes approximately one full week (Huang, 2010). Thus, it is essential to better understand the aerosol behavior and its dispersion process, particularly in remote regions as the tropical Atlantic Ocean where the aerosol data is scarce.

The IX AEROSE expedition took place from Nov 12 to Dec 8, 2013 and its trajectory is illustrated in Figure 3.

This chapter presents the results obtained on the IX AEROSE cruise of 2013, where hourly aerosol measurements were performed to investigate the characteristics and evolution of the aerosol mass distributions.

Figure 3. Cruise track of Nov 12- Dec 8, 2013 cruise

Experimental Methods

For measuring the aerosol mass size distribution, a quartz crystal microbalance (QCM) cascade impactor was used. A picture showing this instrument is provided in Figure 4. The model, PC-2H, has 10 stages corresponding to particle size cut-off points: 0.05, 0.1, 0.2, 0.3, 0.5, 1.0, 2.0, 3.0, 5.6, and 10 μm. Each stage has two quartz crystals as collection surface as depicted on Figure 5; the first one is placed close to the nozzle for collecting particles (sensing) and the second one is used as

reference or control. For this model, the airflow rate is 2 standard liters per minute (slpm), which transports particles through the different stages.

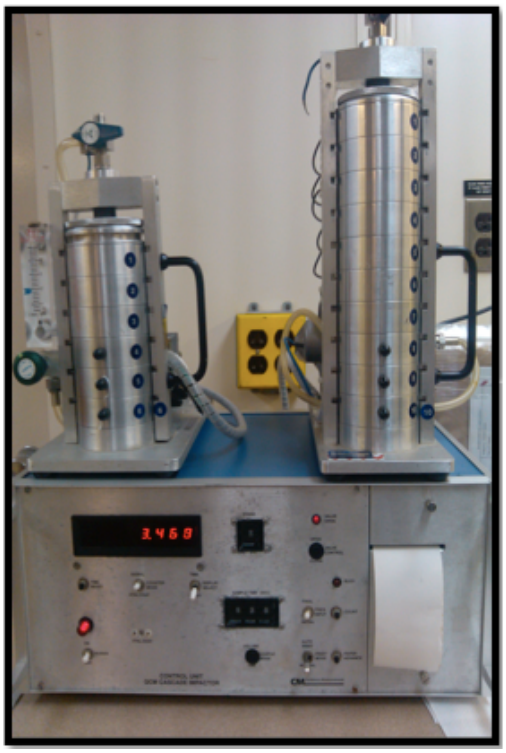

Figure 4. The six stages model (left) and the ten stages (right)

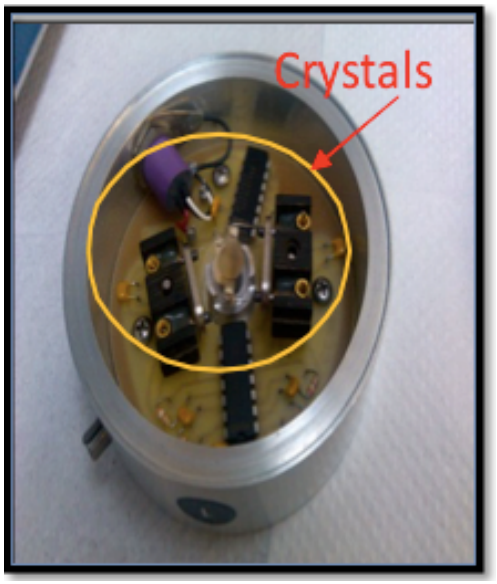

Figure 5. Reference crystal (top-right). Sensing crystal (under the reference to the left)

This device classifies particles by its inertial impact. This means that the most inertial particulate carried in the airflow will impact on the sensing crystal of the first stage, and the lighter ones will continue their way to the second stage; these lightweight particles miss the first crystal and continue with the airflow because of their lower inertial mass. This process is repeated in each stage through the last one, where the smallest particles are collected.

As showed in figures 6 and 7 the nozzle diameters decrease as the number of stages increase from stage 1 to 10; however, in the last two stages not only

decrease the nozzle diameter, but also is added a specific space distribution. This structure allows the particle classification in this cascade impact model.

Figure 6. Decrease of nozzle diameter as the number of stages increases

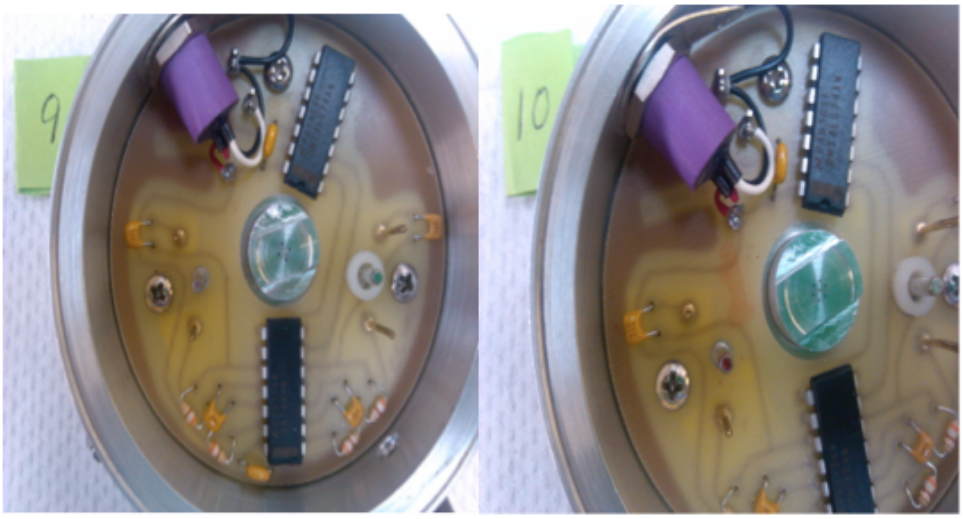

Figure 7. More than one nozzle and a specific space distribution

Thus, the first stage collects particles greater than or equal to 10 μm, the second stage accumulates the particles which diameter is less than 10 μm and greater than 5.6 μm. Then on the successive stages this process repeats itself until the last stage, where particles which diameter is greater than or equal to 0.05 μm are collected.

The collected aerosol mass on the crystals generates a difference resonance vibration, which is proportional to the mass deposited. This difference in frequency is converted to mass by the following algorithm (California Measurements, Inc., 2002):

$$C = K(\frac{dF}{dT})$$

C- concentration ($\mu g/\text{m}^3$)

K - sensitivity constant

dF - frequency difference (Hz)

dT - sampling time ($seconds$)

Results and Discussion

Figures 8 and 9 show the distribution of aerosol mass concentration measured in an hourly basis during Dec 2, 2013. The distributions tend to be unimodal during the morning through mid-day 00:06-12:46 UTC (UTC, Coordinated Universal Time). The graphs exhibit the presence of only one peak value between 0.00562 and 0.01831 µg/m³ in the range of 0.5-1.0 µm of aerodynamic equivalent diameter, as denoted by figures 8a, 8b, 8c, 8d, and 9a.

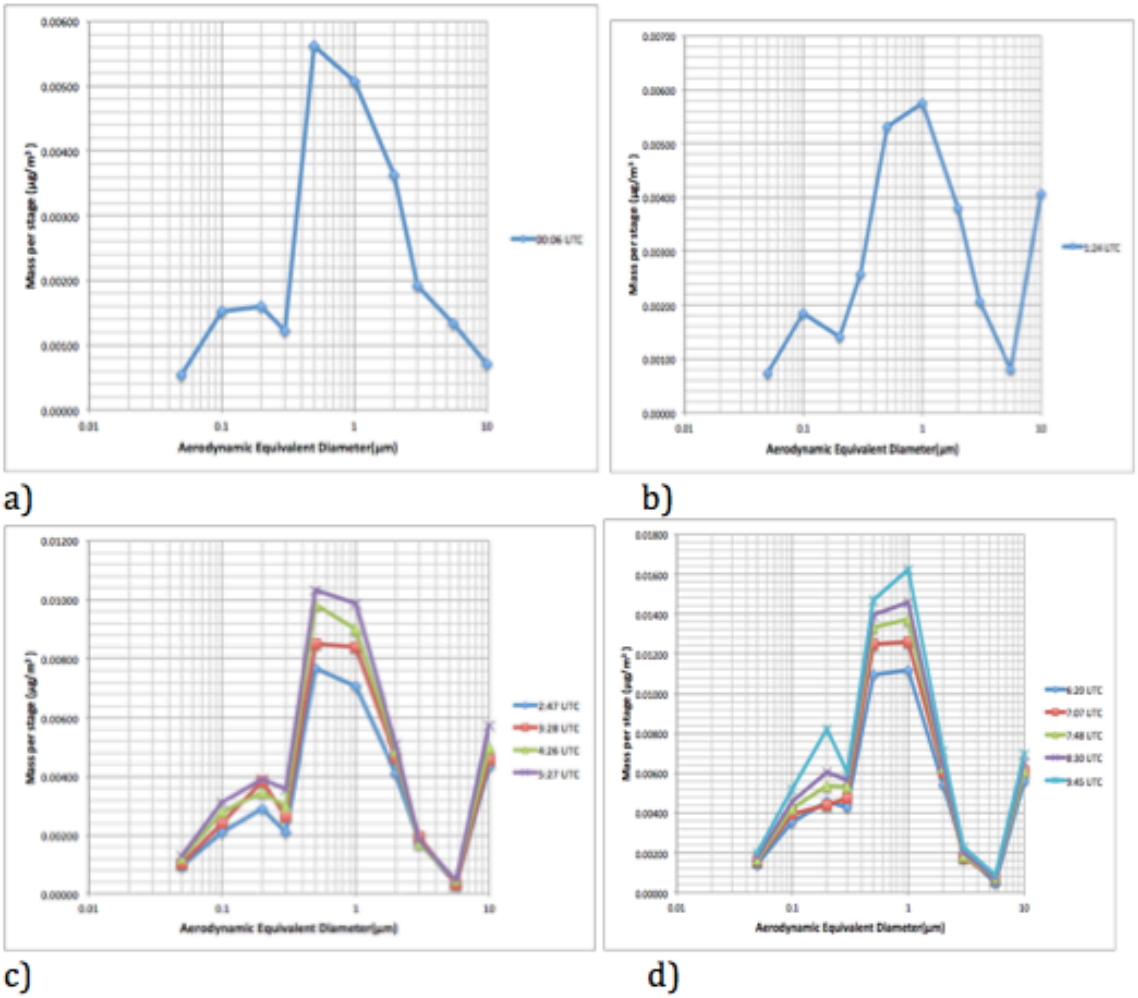

Figure 8. Aerosol mass concentration distribution for 6:00 to 9:46 UTC

Early in the afternoon the distribution becomes bimodal and remains such through the beginning of the evening as shown in Figure 9b. The two peaks are close in height, however one remains a little higher than the other. The peak value decreases by 93% from 0.01831 µg/m³ measured at 12:46 UTC to 0.00118 µg/m³ at 13:50 UTC. Then the maximum peak slowly increases until it reaches a

value of 0.01258 µg/m³ at 23:41 UTC, which is 69% of the peak daytime value, as depicted in Figure 9c.

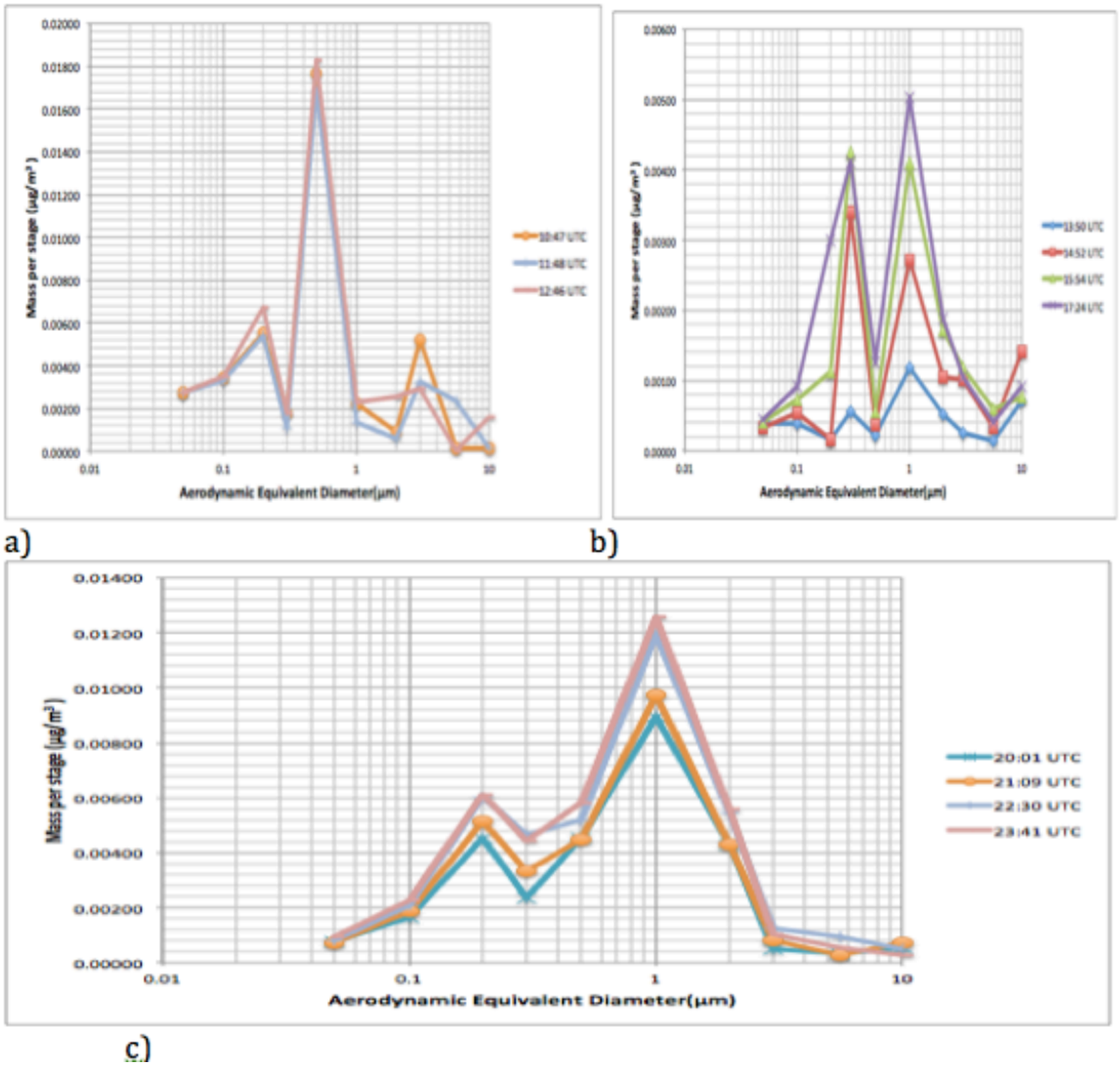

Figure 9. Aerosol mass concentration distribution for 10:47 to 23:41 UTC

Since the distribution shape was variable through the day, the mean mass concentration distribution was determined to define the type of mass distribution that was predominant on that day.

As illustrated in Figure 10a, the maximum in the mass distribution is located in the accumulation region, which is defined by particle diameters between 0.1 and 2.0 µm.

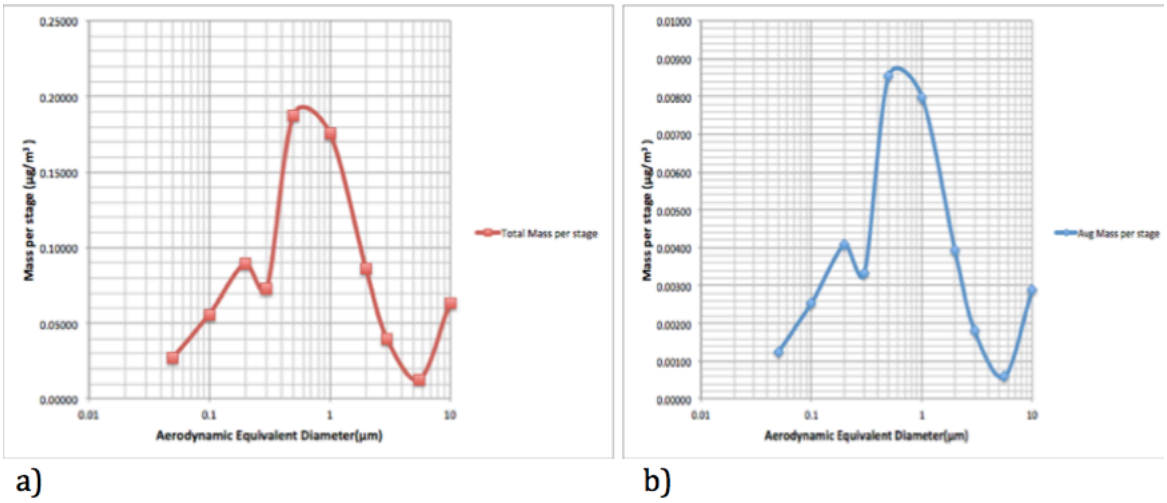

a) b)

Figure 10. Total (a) and average (b) aerosol mass distribution

This is the size characteristic of combustion products (Baron, 2011). Thus, it suggests that the air mass was composed of smoke particles, which generated a unimodal aerosol mass concentration distribution with a total mass density of

0.18794 μg/m³ at 0.5 μm. This finding is important because it allows the determination of the type of the air mass.

Figure 10b represents the mean distribution of the mass concentration. As observed, the average distribution shape follows the same pattern as the total mass distribution. It might suggest that either the 0.5 μm size fraction dominates the mass distribution or it is correlated with the dominant fraction.

Table 1 presents the mean, total mass concentration, and the extreme values for each stage. It can be seen from these data that the nucleation mode is covered by only one stage of the QCM model used in this study; however, the accumulation and coarse modes have six and three stages respectively.

Table 1. Aerosol statistics

Size (µm)	Total Mass/Stage (µg/m$^{3)}$	Mean (µg/m3)	Std. Dev.	Min (µg/m3)	Max (µg/m3)
0.05	0.02723	0.00124	0.00077	0.00032	0.00275
0.1	0.05591	0.00254	0.00133	0.00038	0.00518
0.2	0.08958	0.00407	0.00217	0.00016	0.00819
0.3	0.07291	0.00331	0.00154	0.00056	0.00607
0.5	0.18794	0.00854	0.00573	0.00022	0.01831
1	0.17569	0.00799	0.00459	0.00118	0.01621
2	0.08622	0.00392	0.00205	0.00052	0.00712
3	0.03962	0.00180	0.00104	0.00026	0.00523
5.6	0.01316	0.00060	0.00050	0.00000	0.00234
10	0.06335	0.00288	0.00255	0.00014	0.00693

On average, the accumulation particle mass represented 75% more than nucleation, and 65% more than coarse mode. Therefore, the total aerosol mass is

0.02723 μg/m³ for the nucleation mode, 0.66825 μg/m³ for the accumulation, and 0.11613 μg/m³ for the coarse mode. The maximum extreme values show an increasing tendency of 84% as the mode type change from nucleation to coarse mode.

To corroborate that for the selected day the aerosol particles obtained were smoke, two aerosol forecast models were used: Navy Aerosol Analysis and Prediction System (NAAPS) and the NOAA Environmental Modeling System (NEMS) Global Forecast System (GFS) Aerosol Component (NGAC). Figure 11 and 12 show the 0Z, 6Z, 12Z, and 18Z forecast performed by NAAPS for Dec 2, 2013. Smoke was predicted for the region where the ship was located, which confirms the in-situ measurements.

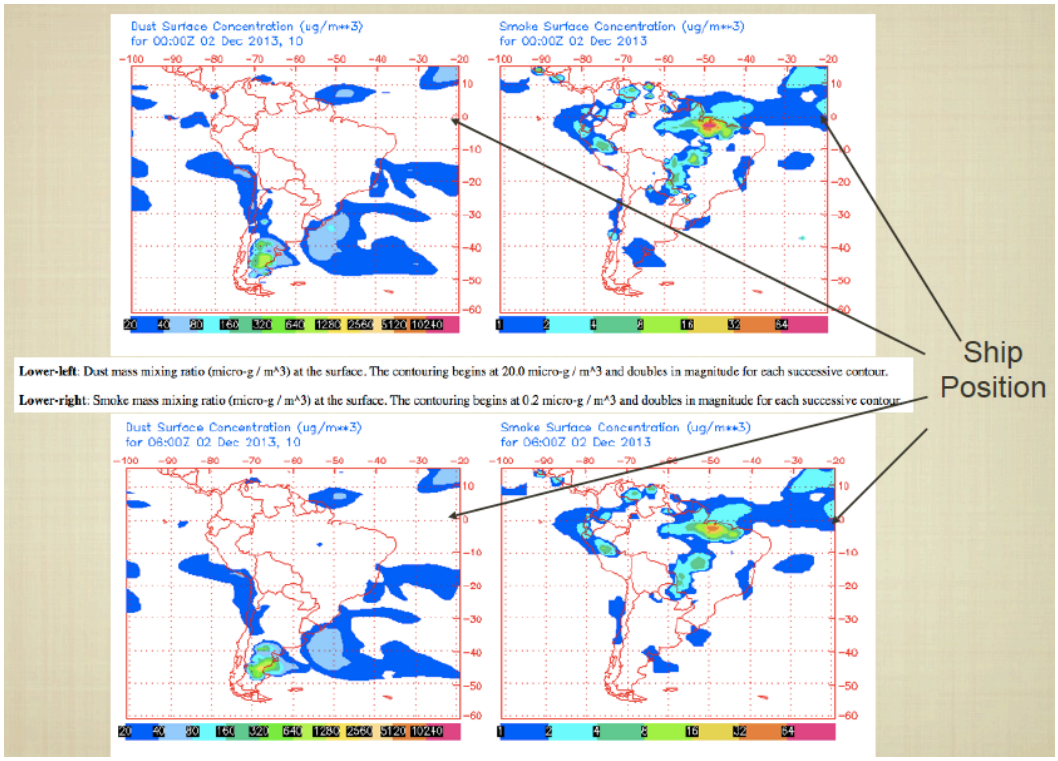

Figure 11. NAAPS forecast for Dec 2, 2013 0Z & 6Z

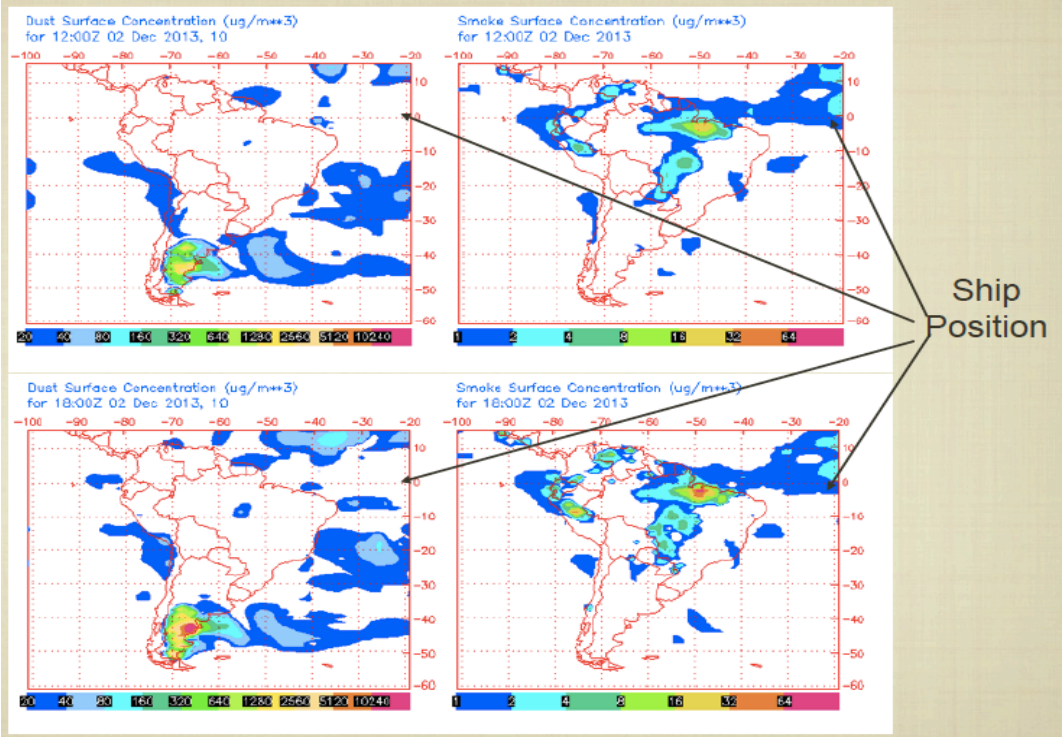

Figure 12. NAAPA forecast for Dec 2, 2013 12Z & 18Z

Figure 13 presents the NEMS GFS Aerosol Component (NGAC) forecast, which at least does not predicts dust conditions for the location where the ship was situated.

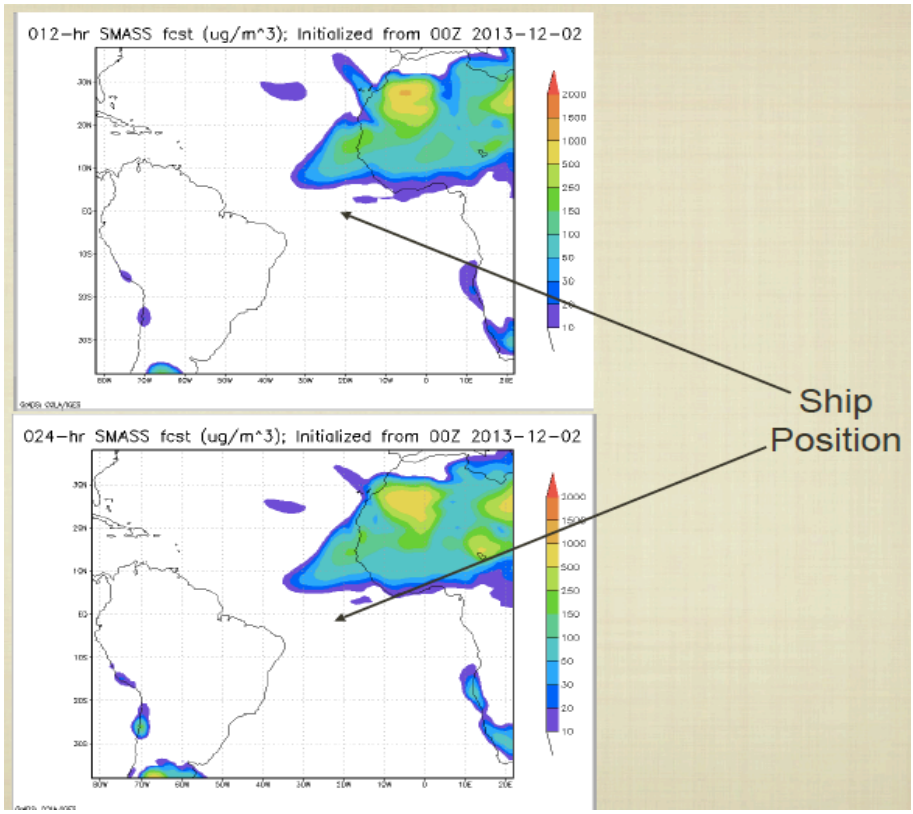

Figure 13. NEMS GFS Aerosol Component forecast

The time series of the mass density is shown in Figure 14, which shows the aerosol mass concentration evolution. From the early morning the aerosol concentration increased until it maxi of 0.06953 µg/m³ at 9:45 UTC, then it decreased to 0.00449 µg/m³ over the next four hours and then began to increase again to a value of 0.0359 µg/m³ at 23:41 UTC nearly ten hours later. The mass concentration drop experienced was large, so the Hybrid Single Particle

Lagrangian Integrated Trajectory (HYSPLIT) model (Draxler, 2003) was used to understand the temporal behavior of the aerosol mass concentration observed.

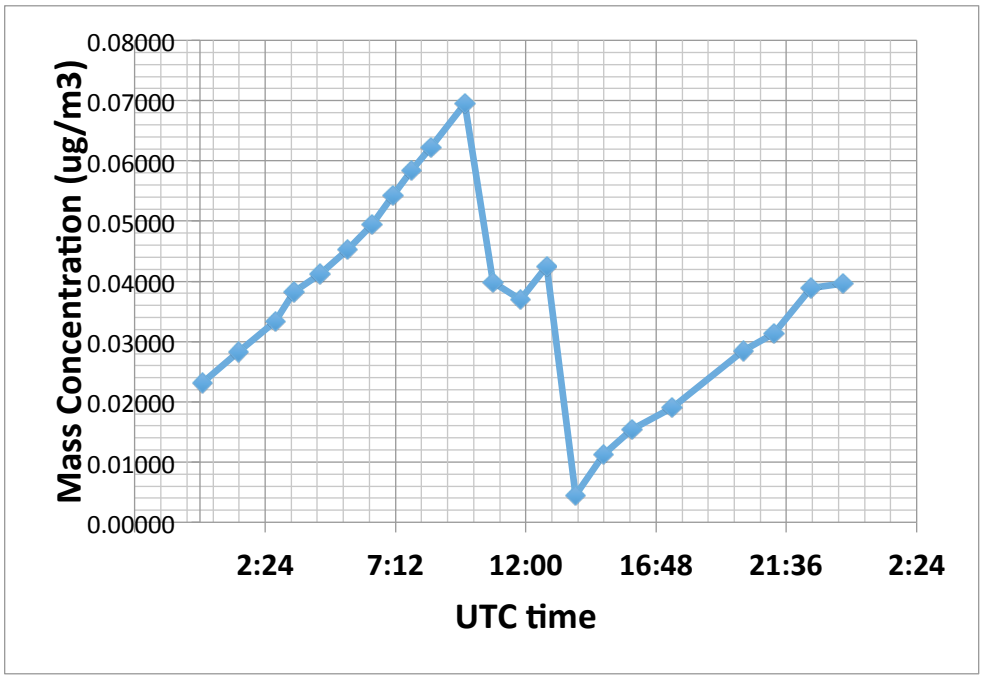

Figure 14. Aerosol mass time series

Figure 15 depicts the Hysplit model, where origins and trajectories of the air masses that were sampled at the ship position are shown. The air masses encountered at 9:45 UTC appear to have originated from the border among Chad, Sudan, and Central African Republic central Africa, when the mass concentration value was at its maximum 0.06953 μg/m³. Three hours later the air masses

arriving at the ship still appeared to have the same source region but the measured mass concentration was at its minimum value of 0.00449 μg/m³. Consequently, the decrease in the measurement value is attributed to the ship's change in direction and not by the winds, as confirmed by the ship's log.

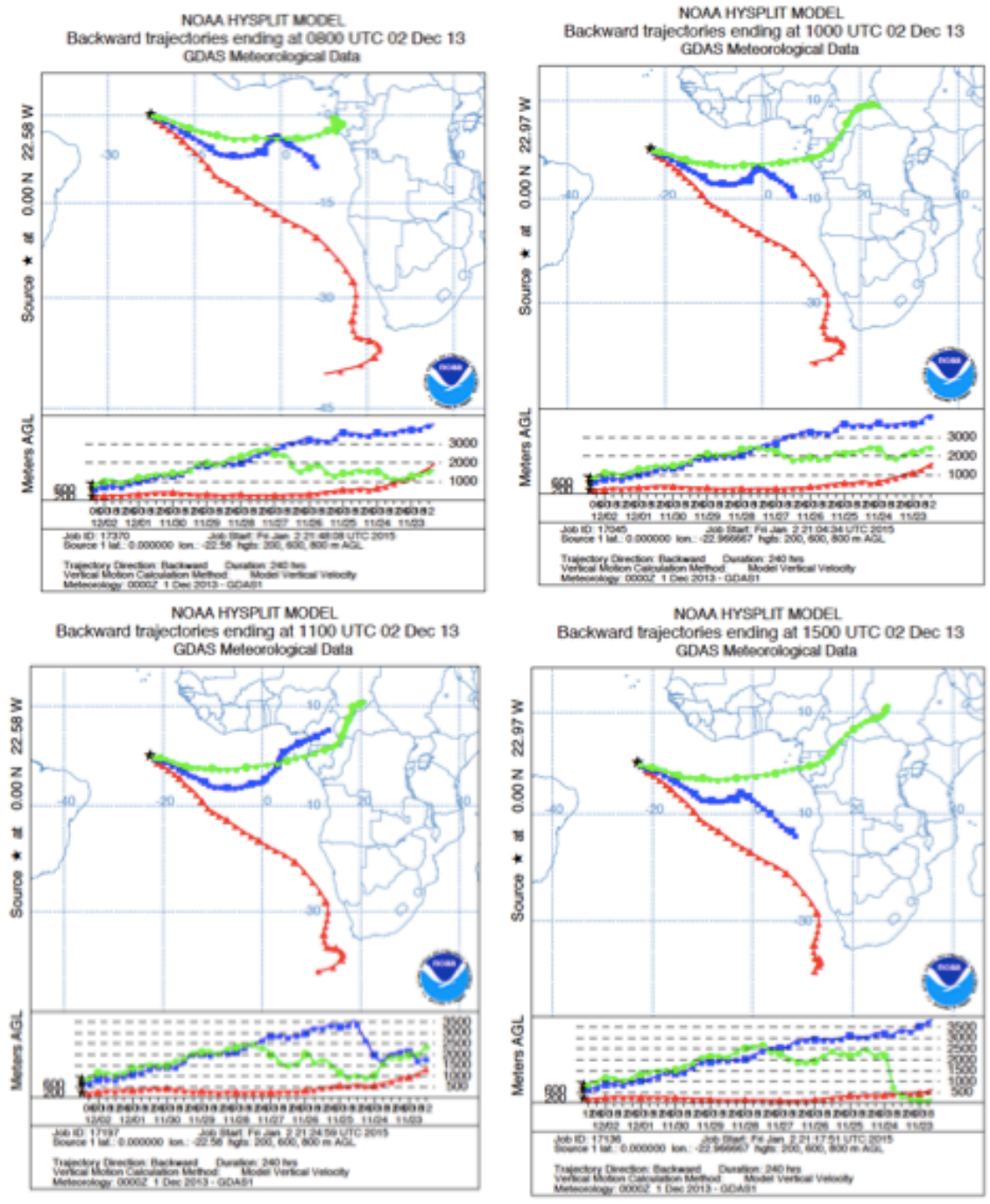

Figure 15. Hysplit air mass analysis model

This kind of situation is not likely to happen in land, where all measuring devices are stationary, but this is one of the issues that could be faced when measuring in remote regions, such as tropical Atlantic Ocean.

The ten days back trajectory analysis denotes that the 600 m air mass outflows from Gabon at 8Z; then it was coming from the border among Chad, Sudan, and South African Republic at 10Z. One hour later, the 400 m air mass has its origin in Cameroon, and the 600 m air mass was coming from the border between Chad and Central African Republic.

Finally, the 600 m air mass was coming from Sudan at 15Z. This reinforces the idea that the smoke aerosol particles originated from combustion since such practice is very common in this region, as it is confirmed by the Moderate Resolution Imaging Spectroradiometer (MODIS) satellite fire map (Fig. 16). This 10-day period fire map collects the places, where fires are detected by MODIS on board the Terra and Aqua satellites. The yellow color denotes a large number of fires. As is depicted by the map, the yellow color is more preponderant over the central African countries already mentioned.

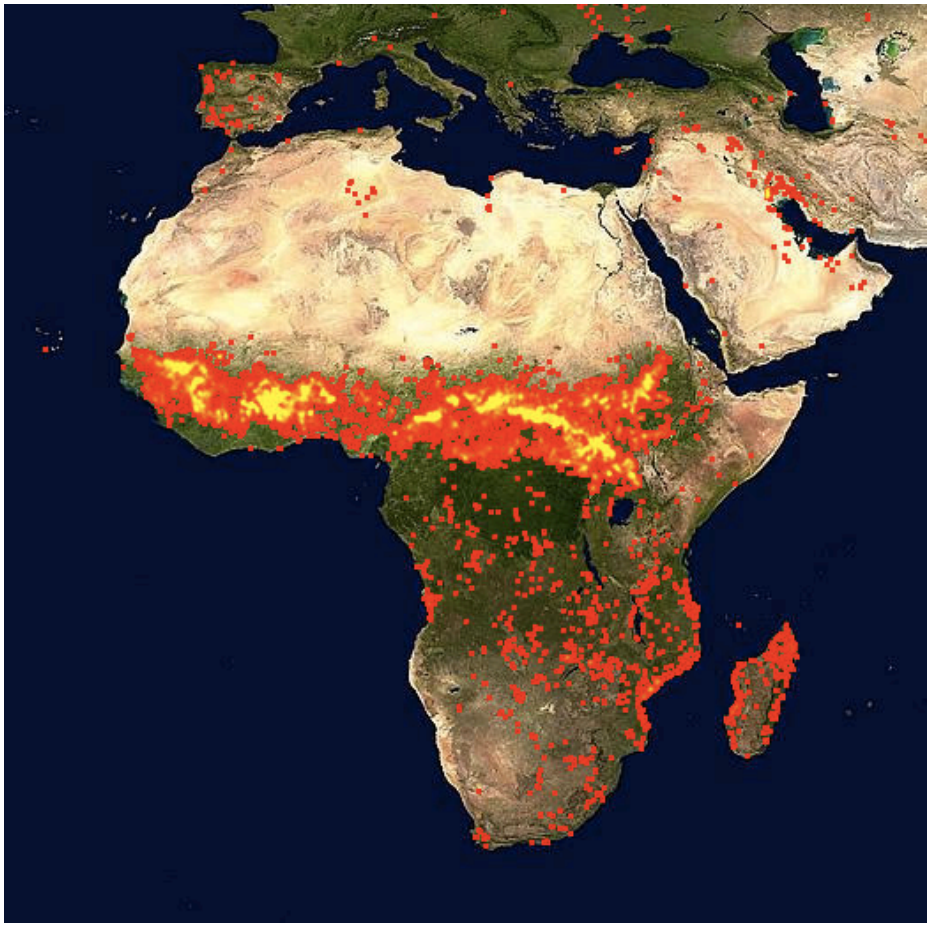

Figure 16. MODIS fire map for Nov 27-Dec 6, 2013 (Modis Web)

In addition, it should be taken into consideration that the distances between the inland emission sources and the ship's position allowed for mixing and interaction as well as condensation and coagulation.

Figure 17 visualizes how Dec 2 looked during the sunset. As can see, a haze of smoke is in the horizon.

Figure 17. Sea smoke sunset on Dec 2

Summary

Atmospheric aerosol mass size distributions were measured directly with a California Instruments Model PC-2H Quartz Crystal Microbalance (QCM). Hourly, size-segregated mass distributions of suspended Saharan dust particulate were obtained for the IX AEROSE expedition on Nov -Dec 2013. The corresponding values of average mass for accumulation, nuclei and coarse mode obtained were: 0.00124±0.000769, 0.00506±0.00254, and 0.00176±0.00114 µg/m³.

The shape of this distribution suggests that the air mass is composed of smoke particles, which was also confirmed by the models used. These smoke particles

have their origin in the African continent as obtained by the backward-trajectory analysis.

This result implies that a relationship between the shape of the mass distribution and the type of the aerosol (dust or smoke) present in the atmosphere can be established and used as an indicator to characterize aerosols.

3. Modal Structure of Aerosol Mass Distribution over the Tropical Atlantic Ocean (Observed During Saharan Dust Episodes)

Since the Intergovernmental Panel on Climate Change (IPCC) Four Assessment Report (AR4), climate models have been incorporating more cloud and aerosol processes as well as their interactions (IPCC Fourth Assessment Report: Climate change 2007 (AR4), 2007). However, significant uncertainties still exist in the accuracy of the models. These uncertainties should be removed with more experimental data validation obtained from field programs such as AEROSE expeditions (AEROSE, 2015) and more recently CalWater2 campaign (Calwater, 2015).

Aerosol particles and their interactions with clouds have forcing effects on climate of -0.9 Wm^{-2}, which have significantly balanced the global mean forcing of greenhouse gases (IPCC Fourth Assessment Report: Climate change 2007 (AR4), 2007). The particle diameter range of atmospheric aerosols which has the most sensitivity to light scattering is between 0.1 and 1 μm, the submicron size range (Hillamo, 2001). The scattering effect will vary depending on the mean diameter,

the mass concentration of the particles, and index of refraction. Several studies (Berner A. , 1980); (Pugatshova, 2007); (Hillamo, 2001); (Berner A. , 1996) have focused on understanding the modal structure of aerosol distributions to better quantify the scattering impact of atmospheric aerosols on climate and to validate models.

This chapter presents the results obtained on the IX AEROSE cruise of 2013, where daily aerosols measurements were performed during Dec 1-4 to assess the modal structure of the aerosol mass distributions over the marine boundary layer of the tropical Atlantic Ocean, using a cascade impactor which is a direct mass concentration measuring method.

Experimental Methods

Quartz Crystal Microbalance Cascade Impactor (QCM) measurements were performed together with other aerosol particle techniques such as Laser Particle Counter (LPC), Scanning Mobility Particle Sizer (SMPS), and Aerodynamic Particle Sizer (APS) during the IX AEROSE expedition (Morris, 2006).

Ambient aerosol mass size distributions were measured directly with a California Instruments Model PC-2H QCM. Impactor measurements were carried out starting on Nov 14 at latitude 17°N and longitude 47°W and ending on Dec 4 at

latitude 6°N and longitude 23°W. The number of impactor measurements performed per day varied from a minimum of 4 on Nov 14 to a maximum of 23 on Dec 30 for a total of 316 replicas of which 137 were performed during the night.

Two different impactor measurement methodologies were applied from Dec 1 to Dec 4. One of the measurement methodologies consisted of getting the data directly from the reading display, and in the second one the data was obtained from the printed reading. This study is based on the printed readings.

Results and Discussion

The total mass concentration as well as the average mass, the extreme values, and the standard deviations per each day are presented in Table 2 for accumulation and coarse mode, but only the total mass concentration values for nucleation mode.

As the ship moved south, the measured total mass concentration decreased slowly from 1.07684 μg/m³ for Dec 1, to 0.81161 μg/m³ for Dec 2, then from 0.65681 μg/m³ for Dec 3 to 0.35705 μg/m³ for Dec 4.

Table 2. Mass concentration per days

		1-Dec		
	Total Mass	Nuclei	Accumulation	Coarse
ΣMass	1.07684	0.07791	0.87657	0.12236
Mean	0.00538	0.00390	0.00730	0.00204
Max	0.03387	0.00798	0.03387	10.00000
Min	0.00000	0.00028	0.00000	0.00028
Std. Dev.	0.00598	0.00276	0.00695	0.00091
		2-Dec		
	Total Mass	Nuclei	Accumulation	Coarse
ΣMass	0.81161	0.02723	0.66825	0.11613
Mean	0.00369	0.00124	0.00506	0.00176
Max	0.01831	0.00275	0.01831	0.00693
Min	0.00000	0.00032	0.00016	0.00000
Std. Dev.	0.00369	0.00077	0.00402	0.00185
		3-Dec		
	Total Mass	Nuclei	Accumulation	Coarse
ΣMass	0.65681	0.01517	0.60443	0.03721
Mean	0.00597	0.00138	0.00916	0.00113
Max	0.02589	0.01517	0.02589	0.00194
Min	0.00000	0.00000	0.00048	0.00007
Std. Dev.	0.00596	0.00073	0.00580	0.00055
		4-Dec		
	Total Mass	Nuclei	Accumulation	Coarse
ΣMass	0.35705	0.01016	0.29590	0.05099
Mean	0.00151	0.00053	0.00308	0.00087
Max	0.00188	0.00182	0.01592	0.00329
Min	0.00000	0.00000	0.00000	0.00000
Std. Dev.	0.00188	0.00060	0.00308	0.00087

The aerosols were transported by air masses coming from the southeast Atlantic and western African continent, as showed by the HYSPLIT back trajectory analysis of surface winds at 200, 400, and 600m (Fig. 18-21).

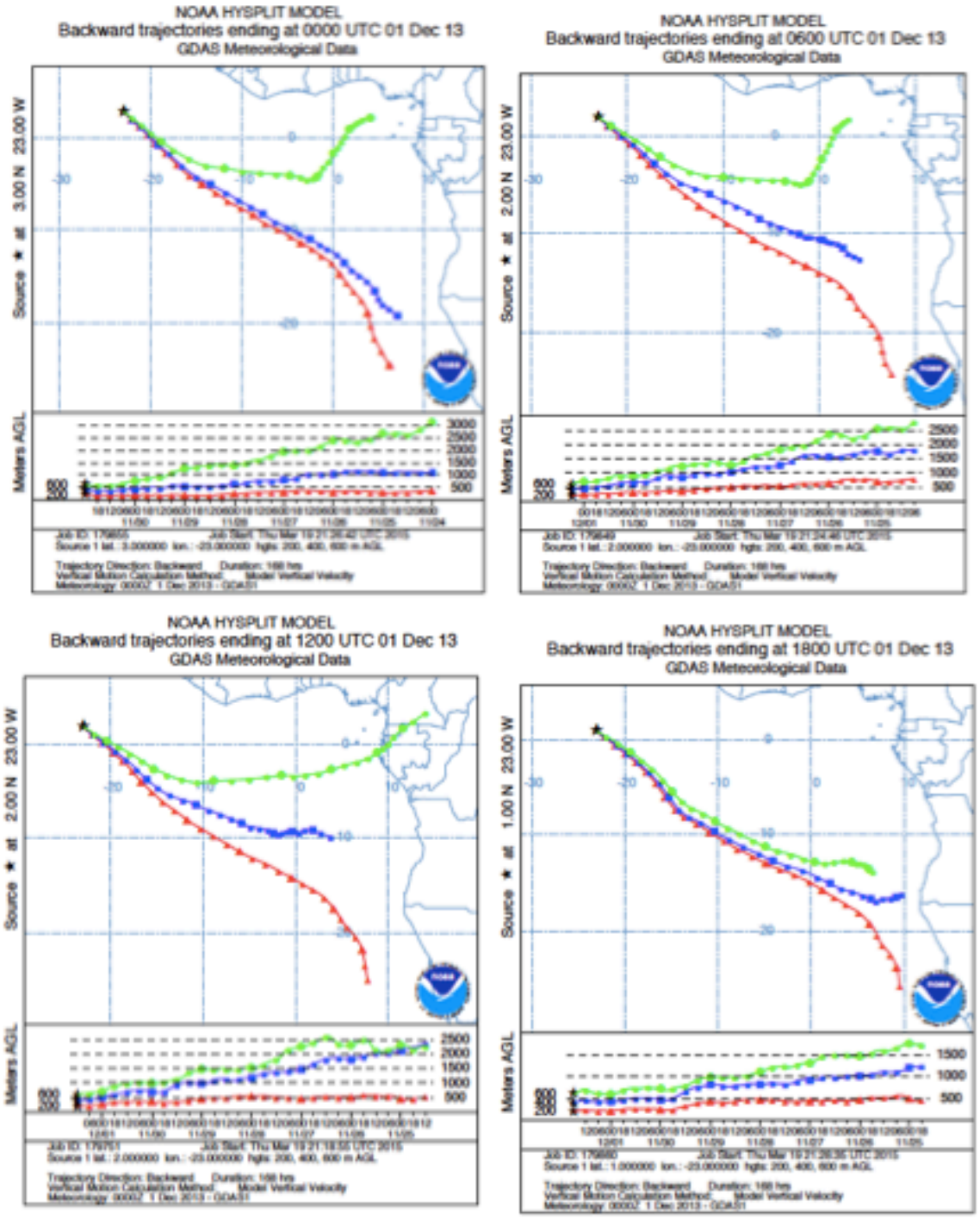

Figure 18. Dec 1 backward trajectory analysis of surface air

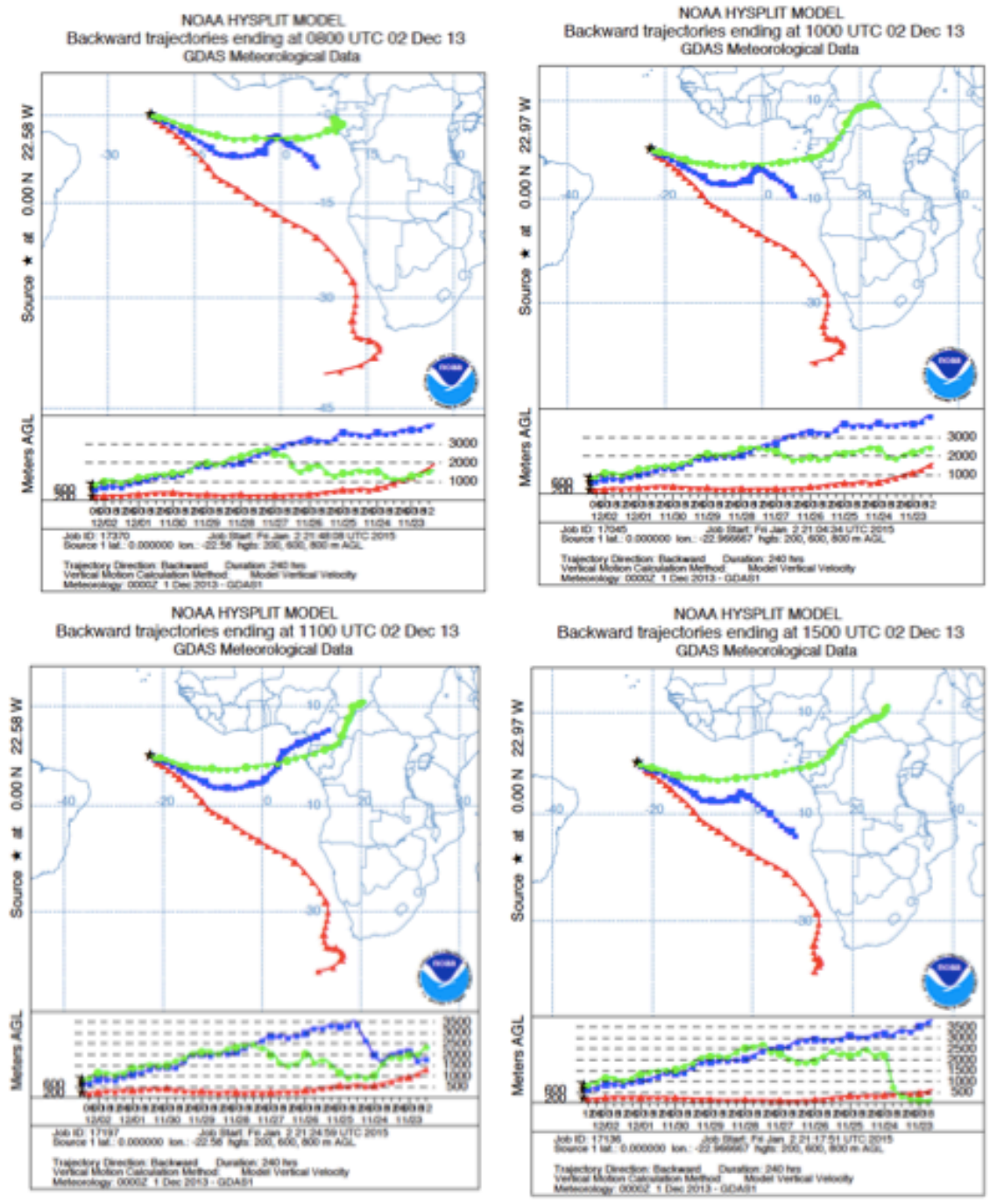

Figure 19. Dec 2 back trajectory analysis of surface air

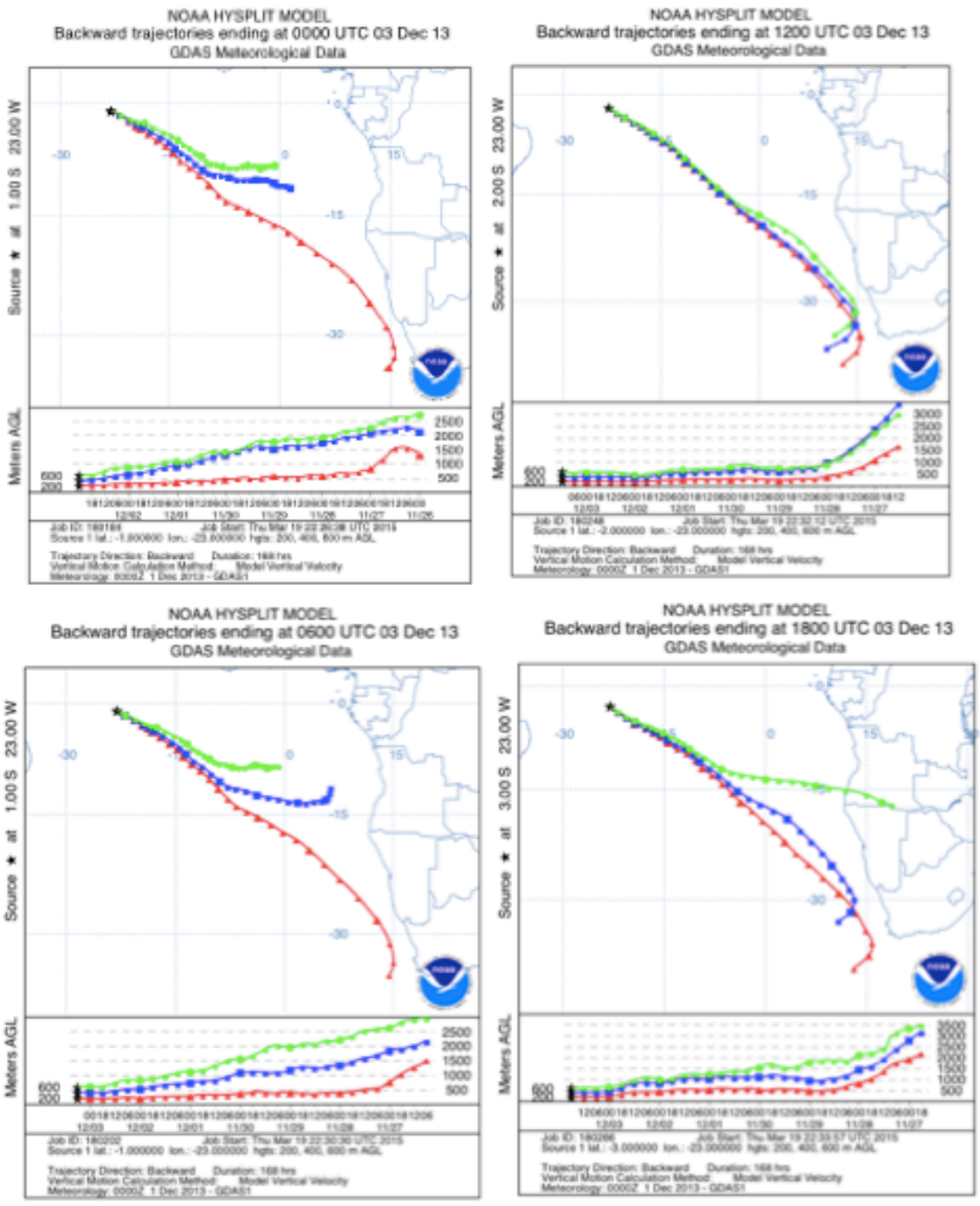

Figure 20. Dec 3 back trajectory analysis of surface air

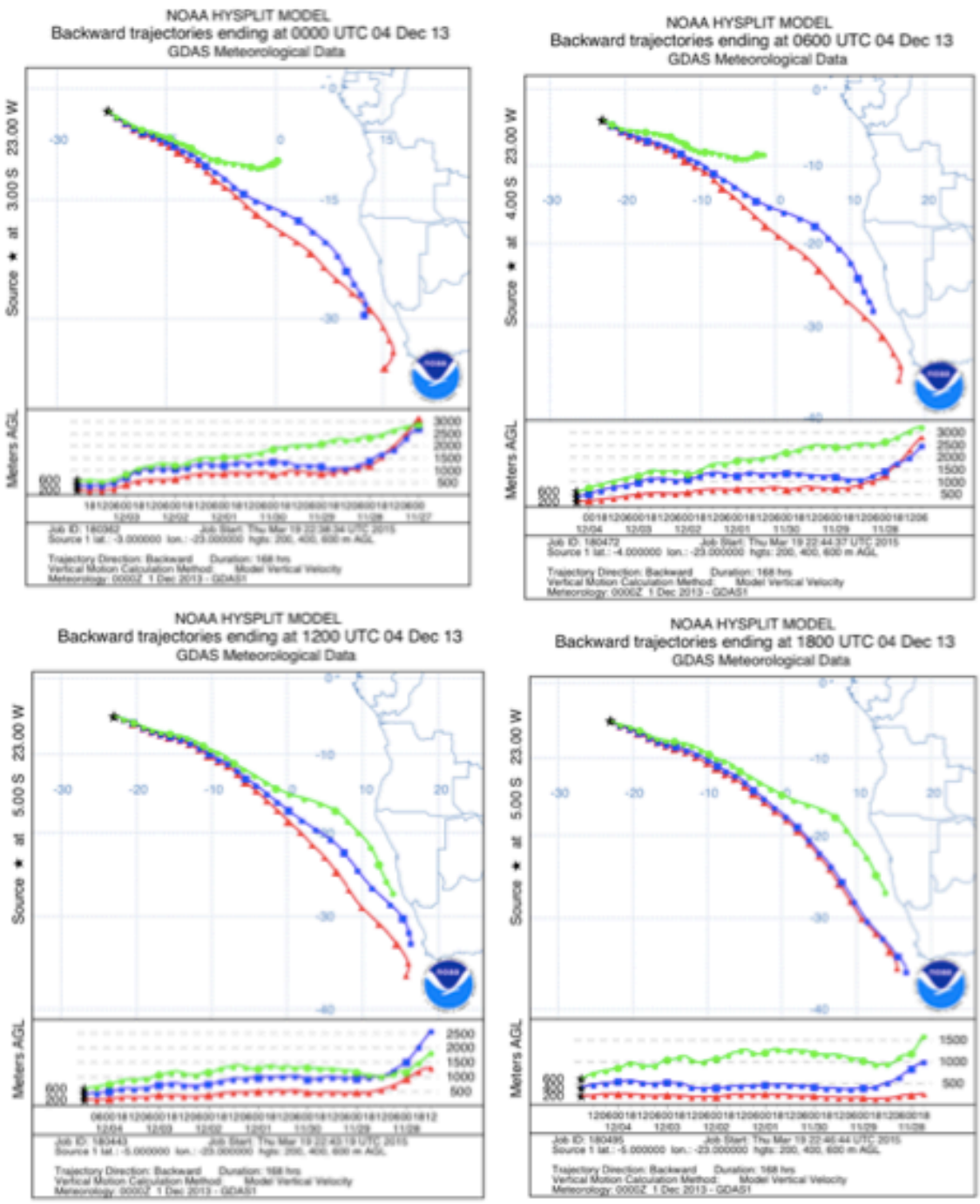

Figure 21. Dec 4 back trajectory analysis of surface air

The HYSPLIT analysis looked back for a week, hence the aerosols transported by air masses at 200 and 400 m had experienced an aging process, having undergone condensation and coagulation growth over the marine boundary. A similar process had been experienced by the air masses at 600 m, originating from the western African continent at a height over 2500m.

During these four days, the ship traveled south along 23°W (Table 3) and the measured average mass concentration decreased by 25% from Dec 1 to Dec 2, 19% from Dec 2 to Dec 3, and more than 45% from Dec 3 to Dec 4.

Table 3. Ship coordinates through Dec 1-4

Date	Time	Latitude	Longitude
12/1/13	0z	3	-23
	6z	2	-23
	12z	2	-23
	18z	1	-23
12/2/13	0z	1	-23
	6z	0	-23
	12z	0	-23
	18z	0	-23
12/3/13	0z	-1	-23
	6z	-1	-23
	12z	-2	-23
	18z	-3	-23
12/4/13	0z	-3	-23
	6z	-4	-23
	12z	-5	-23
	18z	-5	-23

The standard deviations for the average total mass values are quite large, as well as the difference between the extreme values, which is explained by the very large difference mass concentrations measured among the three modals, as shown in Figure 22.

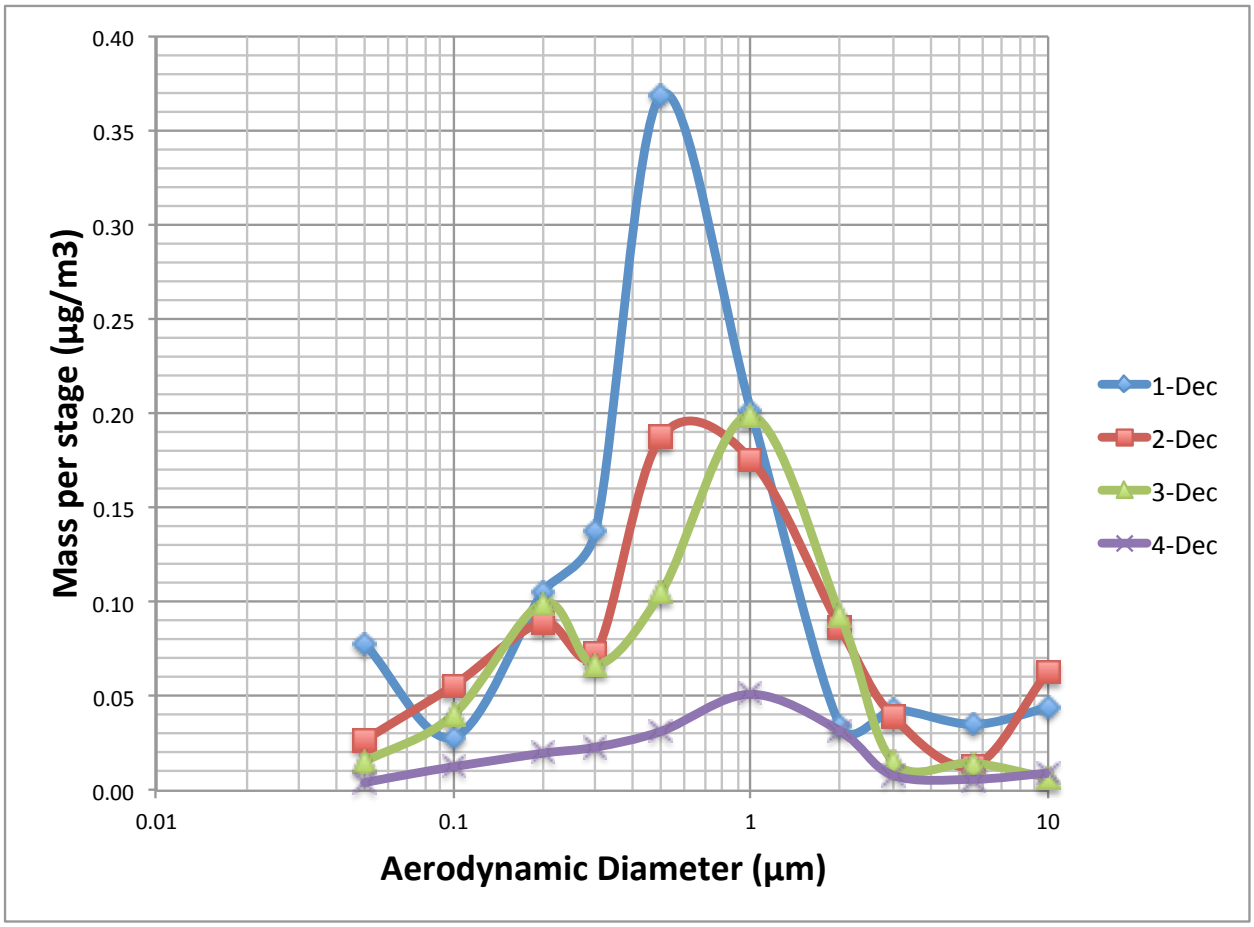

Figure 22. Aerosol mass distribution for Dec 1-4

Nucleation

The nucleation mode data is partial because the reduced measuring range of this QCM model. It has only one stage, which represents the nucleation mode, as represented in Table 4.

The particle origin of this mode, in urban sites, is basically from the coagulation and condensation of supersaturated combustion vapor, and its contribution to the total mass is low (Airborne Particle, 1979). Being on the ocean, the nucleation particle's origin is due to gas-to-particle conversion mechanisms such as homogeneous nucleation, heterogeneous nucleation, and condensation (Lewis, 2004); however, the mass of this particle mode is an insignificant percent of the total mass. Accordingly, the measured nucleation total masses were 0.07791 $\mu g/m^3$, 0.02723 $\mu g/m^3$, 0.01517 $\mu g/m^3$, and 0.01016 $\mu g/m^3$ for Dec 1-4, which respectively constituted 7, 3, 2, and 4% of the total mass measured each day.

Table 4. Number of stages per mode

Mode	Stage Size (µm)
Nuclei	0.05
Accumulation	0.1
	0.2
	0.3
	0.5
	1
	2
Coarse	3
	5.6
	10

Accumulation

The measurement range of the cascade impactor Model PC-2H covers the entire accumulation range. The majority of its stages fall into the accumulation range from stage size 0.1 to 2 µm. However, nucleation and coarse modes are poorly

represented, as shown in Table 4. Accumulation mode is completely characterized in this study, and thus, the mass, the modal diameter, and the geometric standard deviation were characterized.

The total mass of accumulation mode was higher on Dec 1, which could be explained by the backtrajectory analysis, in which not only marine air mass was influential over the ship's location, but also a 600 m high air mass was originating from the border between Cameroon and Chad, which increased the aerosol loading. On Dec 2, the 600m height mass contribution was marine air mass most of the day. As the days passed, the total mass decrease, the average mass of accumulation mode decreased about 25% from Dec 1 to Dec 2, 9% from Dec 2 to Dec 3, and more than 50% from Dec 3 to Dec 4.

As illustrated in Figures 23-26, NAAPS forecast model predicted a light smoke plume ranged between 1 and 2 $\mu g/m^3$ for Dec 2-4, but a heavier plume of 2 and 4 $\mu g/m^3$ for Dec 1. This forecast is in agreement with the ship-based measurements, where the Dec 1 measured mass was 25-67% higher than those masses observed on Dec 2-4.

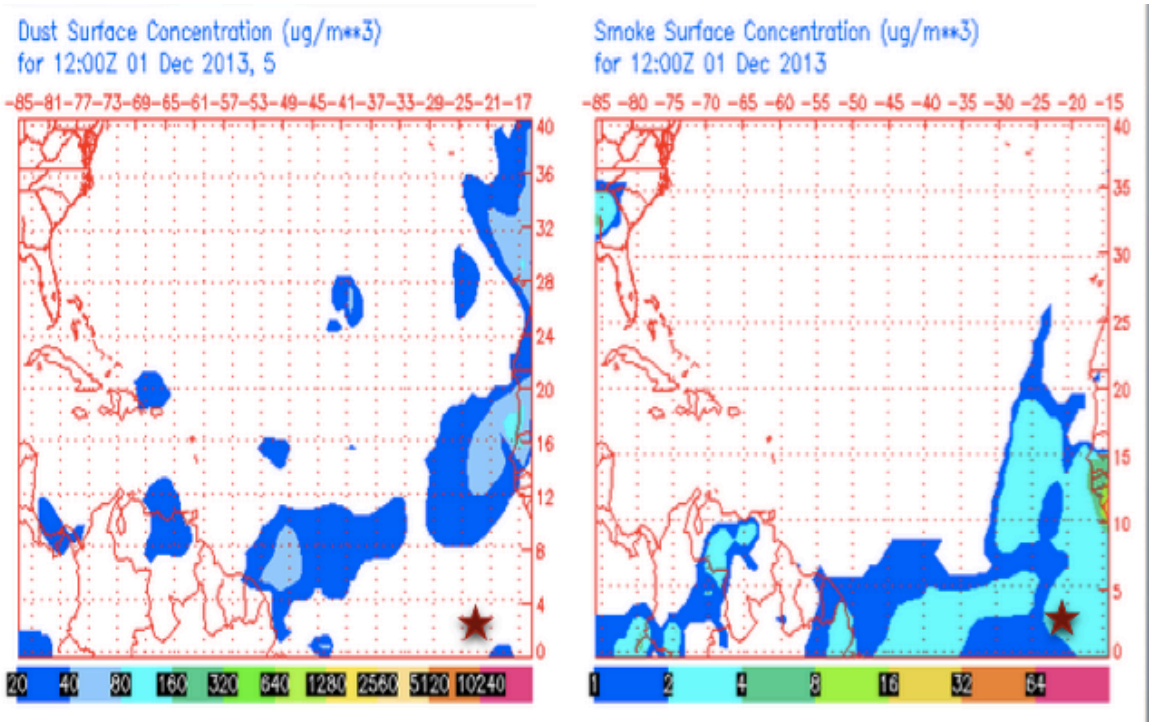

Figure 23. NAAPS dust surface and smoke forecast for Dec 1

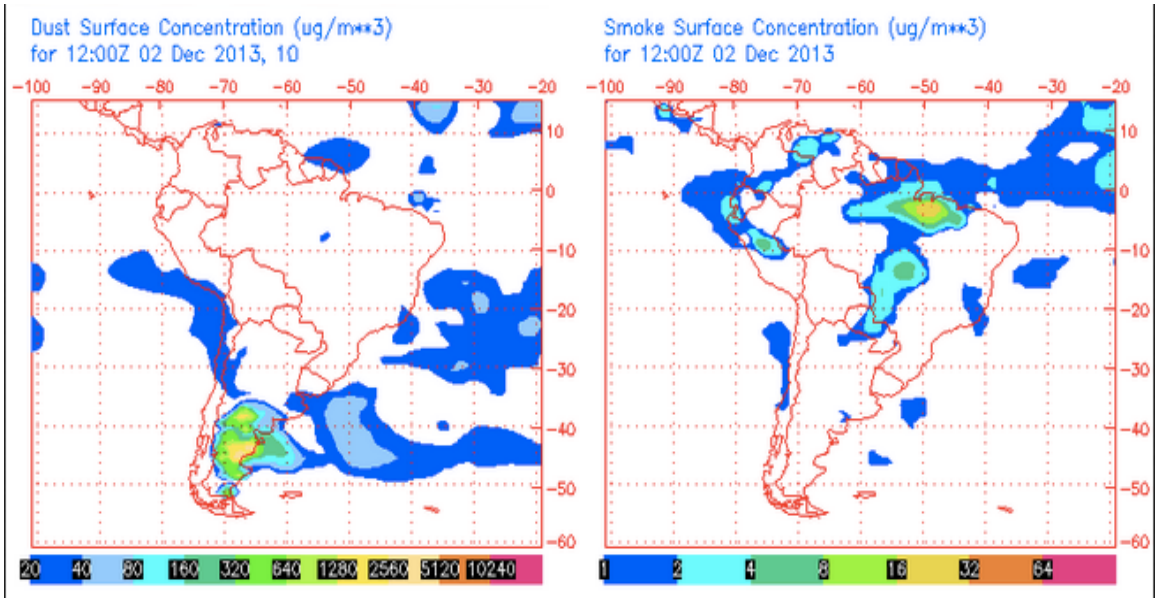

Figure 24. NAAPS dust and smoke surface forecast for Dec 2

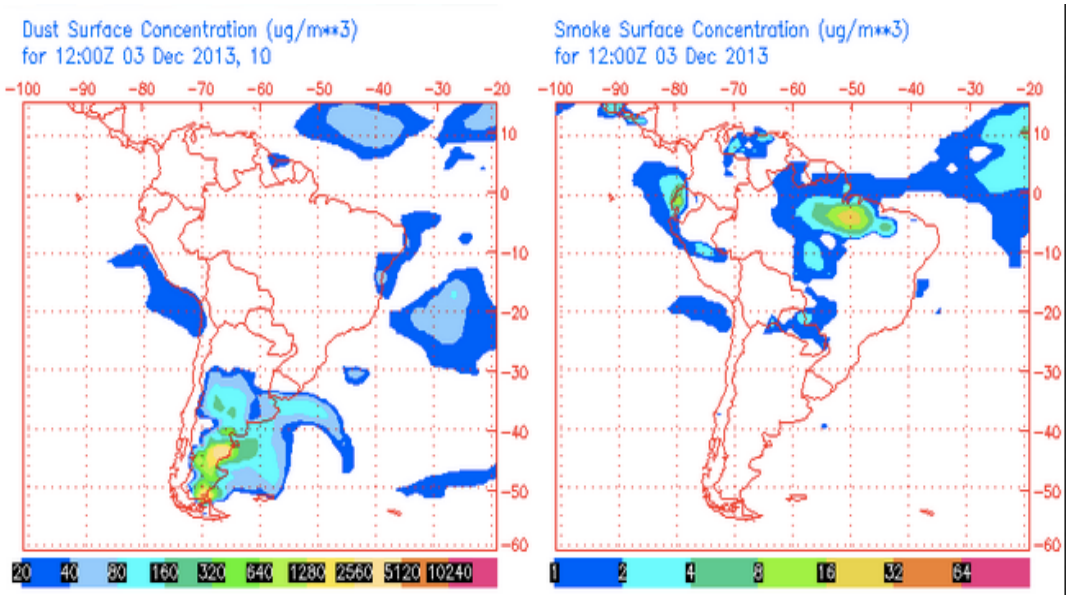

Figure 25. NAAPS dust and smoke surface forecast for Dec 3

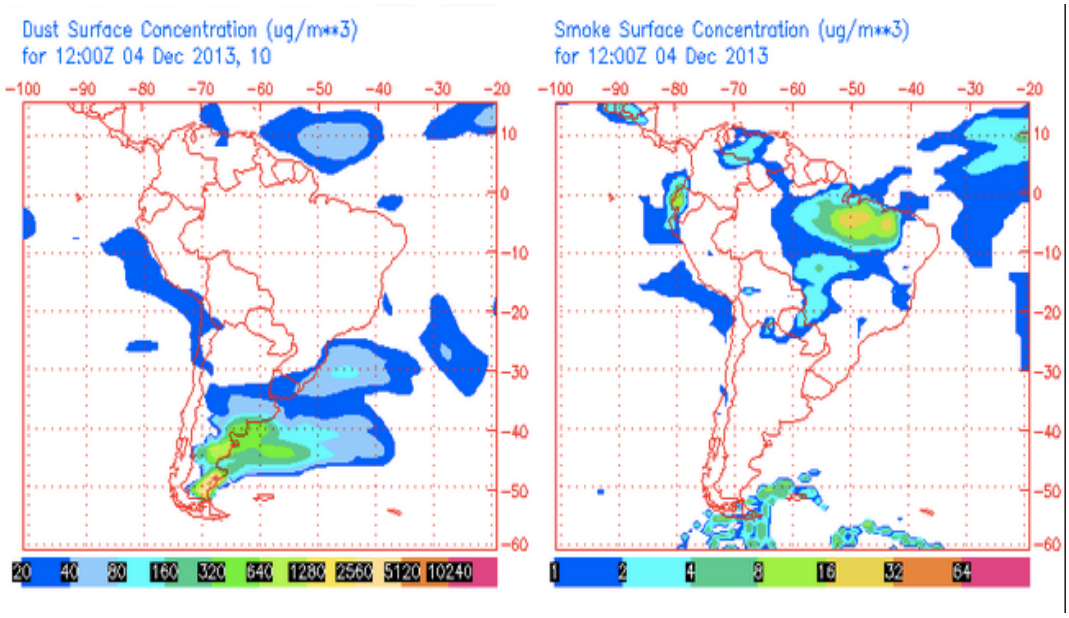

Figure 26. NAAPS dust and smoke surface forecast for Dec 4

Table 5 represents the accumulation modal data, the mass median aerodynamic diameter (MMAD) and the geometric standard deviation of the log normal distribution. The mass median diameters show a high degree of uniformity during Dec 1, 2, and 4 as show the standard deviation values. However, the particle diameter decreases by 16% on Dec 3, and then increases by 20%, which could indicate a greater dimension variability of the measured particles on Dec 3.

Table 5. Mass median aerodynamic diameter (MMAD) and geometric standard deviation for accumulation mode

Day	Diameter (µm)	Standard Deviation
1-Dec	0.68	1.97
2-Dec	0.68	1.62
3-Dec	0.57	2.18
4-Dec	0.72	1.92

Coarse

Although the coarse total mass percent is higher 11, 14, 6, and 14% than the nucleation mode 7, 3, 3, and 4% during the Dec 1-4 measurement period, the coarse mass concentrations are a small portion of the aerosol total mass.

Observing the air mass back trajectories shown in Figure 18-21, it can be seen that the aerosols arriving at the measuring site most often originated over the ocean surface. This excludes the possibility that these air masses were composed of large amounts of continental particles, but which can be composed of sea salt aerosol. The major formation mechanism of which are spray seawater and bubbling air through seawater (Lewis, 2004) and have undergone large mixing processes.

The total mass of coarse mode decreased from 0.12236 μg/m³ for Dec 1, to 0.11613 μg/m³ for Dec 2, then increased from 0.03721 μg/m³ for Dec 3 to 0.05099 μg/m³ for Dec 4, while accumulation mode decreased during the whole period.

Summary

The aerosol modal characteristics over tropical Atlantic Ocean have been evaluated for November-December while the ship traveled south along 23°W between 3°N and 5°S. The obtained aerosol mass distributions have an averaged total mass of 0.00538±0.00598 μg/m³ for Dec 1, 0.00369±0.00369 μg/m³ for Dec2, 0.00597± 0.00596 μg/m³ for Dec 3, and 0.00151±0.0188 μg/m³ for Dec 4. Mass median aerodynamic diameter (MMAD) ranged from 0.57 to 0.72 μm and

geometric standard deviation between 1.62 and 2.18 for accumulation mode, were calculated.

4. $PM_{2.5}$ and Trace Gases analysis over the marine boundary layer of the tropical Atlantic Ocean (Observed During Saharan Dust Episodes)

Dust, smoke, and haze are part of almost any sky horizon in cities and rural zones, as well as in remote areas as the oceans. Since the beginning of civilization, human activities have been polluting the air. But, only in the last two centuries the pollution has became a serious problem because of the rapidly growing population and industrialization.

In general, air quality is worst close to the emission sources such as industrial and traffic-heavy urban areas including our residences since indoor air pollution is a main problem. Many pollutants can be transported by wind long distance, so the pollution is spread to larger areas. Consequently the local air pollution problematic is converted into a regional or continental problem, or even worst a global o hemispheric (De Nevers, 2000). Concern about air pollution is a major issue worldwide today, particularly pollution by trace gases such as carbon monoxide (CO), sulfur dioxide (SO_2), ozone (O_3), and particulate matter with a diameter of 2.5µm ($PM_{2.5}$), because they have a negative impact in health, weather, climate, and natural ecosystem.

Carbon monoxide is a colorless, odorless nonirritating gas, which is extremely toxic to the extent to be asphyxiant. This primary inorganic compound is produced by incomplete combustion of fossil fuels, biomass burning, plant and animal respiratory process, and organic material anaerobic decomposition. CO differentiates from the majority of pollutant for its acute health effects since CO can combines with the hemoglobin and decreases the blood's ability to transport oxygen (De Nevers, 2000).

Sulfur dioxide is a colorless, odor-irritant, and corrosive gas, which oxidation occurs through vary distinct mechanisms such as gas-to-particle conversion, and catalysts (Ondov, 1998). Organic fuels such oil, wood, or natural gas contain sulfur and the burning process of these fuels form sulfur dioxide, which can be deposited mainly over the ocean by acid precipitation (Univerisity of Toledo, 2015). This rain acidifies lakes and streams, damages the vegetation, destroys buildings, statues, and sculptures, as well as contributes to decrease the visibility and harm public health.

Ozone is a colorless, pungent, and highly reactive gas. As a secondary pollutant, it is not emitted into the air directly. It is the principal component of smog, which is caused primarily by automobile emissions, predominantly in urban areas. Distinct

from the stratospheric ozone layer, which lies 10 km above the earth's surface, the pollutant ozone is in the troposphere, which is the lowest major atmospheric layer, and is located from the Earth's surface up to the bottom of the stratosphere. Ground level ozone is formed by photochemical reaction driven by the action of ultraviolet light on the precursor pollutants oxides of nitrogen (NOx) and volatile organic compounds (VOCs). Motor vehicles, power plants, industrial facilities, biomass burning, and lightning produce the NOx. The VOCs is mostly emitted by motor vehicles, vegetation, industrial, and commercial dry cleaners, and paints. In the mentioned photochemical reaction between NOx and VOCs, also it should be present high temperature and low wind speed.

$PM_{2.5}$ are those atmospheric particles, which diameter is less than 2.5μm and belong to nucleation and accumulation modes. These particles arose health concern due to their tiny size. Lon-term exposure to these particles can increase the risk for cardiopulmonary and lung cancer mortality (Hillamo, 2001). $PM_{2.5}$ aerosol particles, once inhaled, can penetrate deep into the whole respiratory system till alveolar region without obstacles, accumulate there and induce different respiratory diseases. Toxic organic compounds and heavy metals that can be originated by burning plants and purifying and processing metals are types of $PM_{2.5}$ (De Nevers, 2000).

This chapter presents an analysis of the characteristic of $PM_{2.5}$ and trace gases: CO, O_3, and SO_2 and explores their behavior from Dec 1 to Dec 4, while the National Oceanic and Atmospheric Administration (NOAA) vessel Ronald H. Brown traveled south along 23°W between 3°N and 5°S over the tropical Atlantic Ocean.

Experimental Methods

The CO, SO_2, and O_3 concentrations were measured in volumetric concentration (ppb) using Thermo Environmental Instruments (TEI). The instruments were located forward at the second level of the ship at 12m high above the sea level (Roper, In preparation). For comparative purposes, the volumetric concentration (ppb) was converted in mass concentration ($\mu g/m^3$) using the following expression:

$$Cm = \left(\frac{PM}{RT}\right) Cv$$

$Cm - mass\ concentration\ (\frac{\mu g}{m3})$

$P - atmosphere\ presure\ (Pa)$

$M -\ molecular\ weight\ (\frac{\mu g}{mol})$

$R -\ \ absolute\ gas\ constant\ [\frac{Pa * m3}{mol * K}]$

$T - temperature\ (°K)$

$Cv - volumetric\ concentration\ (ppb)$

$PM_{2.5}$ mass concentrations were determined using a PC-2H model Quartz Crystal Microbalance Cascade Impactor (QCM) from California Measurements. This instrument performs real-time measurements of mass concentration using vibrating quartz crystal sensor.

The mass concentration data of CO, SO_2, O_3 and $PM_{2.5}$ used for this study was obtained from Dec 1 to Dec 4 while the vessel was traveling south along 23°W between 3°N and 5°S. Two different impactor measurement methodologies were applied from December 1 to December 4. One of the measurement methodologies consisted of getting the data directly from the reading display, and in the second one the data was obtained from the printed reading. This study is based on the printed readings.

Results and Discussion

Table 6 shows the total mass concentration, the mean value, the standard deviation, as well as the extreme values for CO, SO_2, O_3 and $PM_{2.5}$.

Table 6. Mass concentration per days

	1-Dec			
	PM_2.5 (µg/m^3)	CO (µg/m^3)	SO2 (µg/m^3)	O3 (µg/m^3)
ΣMass	0.62152	33414.252	5.163	911.500
Mean	0.03108	1670.713	0.258	45.575
Max	0.05945	1725.047	0.341	49.286
Min	0.00340	1586.648	0.189	42.131
Std. Dev.	0.015	43.085	0.051	2.427
	2-Dec			
ΣMass	0.69548	35922.097	5.350	890.658
Mean	0.03161	1632.823	0.243	40.484
Max	0.05945	1687.884	0.354	43.563
Min	0.00340	1525.686	0.167	36.680
Std. Dev.	0.015	39.728	0.043	2.223
	3-Dec			
ΣMass	0.41971	17962.971	3.062	508.717
Mean	0.03816	1632.997	0.278	46.247
Max	0.05945	1653.834	0.627	48.985
Min	0.01920	1576.396	0.164	40.104
Std. Dev.	0.013	22.808	0.126	2.596
	4-Dec			
ΣMass	0.59190	29980.817	4.494	858.450
Mean	0.03115	1577.938	0.237	45.182
Max	0.05945	1664.818	0.309	49.456
Min	0.00340	1536.487	0.144	38.981
Std. Dev.	0.015	38.502	0.045	3.220

The measured averaged mass of SO_2, O_3, and $PM_{2.5}$ for Dec 1 was respectively 0.258±0.051, 45.575±2.427, and 0.03108±0.015 µg/m^3, which is 0.02, 3, and 0.003 % of the CO averaged mass of 1670.713 ± 43.085 µg/m^3. Figure 27 visualizes the magnitude of the measured CO mass concentration value related to that

measured for SO_2, O_3, and $PM_{2.5}$. For Dec 2-4 a similar measured mass proportion was observed.

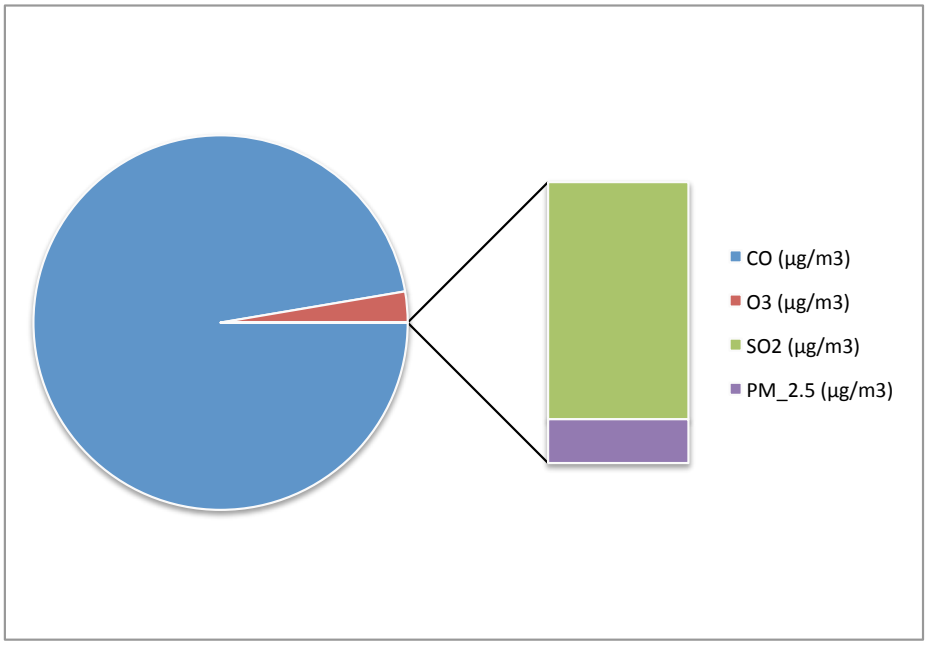

Figure 27. Percent of SO_2, O_3, and $PM_{2.5}$ mass concentration related to CO

Abdus Salam et al. have reported much lower atmospheric trace gas mass concentrations, but over the land (Salam, 2008). Their values of averaged CO concentrations measured at five different locations range between 41.7±5 and 334.2±22 µg/m^3, which is respectively 80 and 97 % less compared to the minimum and maximum mean CO measurements reported in this study for Dec 1. While a study performed by Sayar Yaseen et al. have reported an averaged

monthly SO_2 concentration of 21±2.88 μg/m^3 measured in a village located close to Parichhna thermal power plant (Yaseen, 2014). This value of 21±2.88 μg/m^3 is 99% higher that 0.237±0.045 μg/m^3 the lower mean SO_2 concentration value measured on Dec 4.

Figure 2 shows how associated was the CO with the $PM_{2.5}$ for the four days under analysis. A positive, but weak correlation was observed as denote the correlation coefficient values of: 0.028 for Dec 1, 0.0003 for Dec 2, 0.285 for Dec 3, and 0.079 for Dec 4. Being Dec 3 the day with the lower $PM_{2.5}$ and CO mass concentration value, but with the strongest correlation, where R^2=0.285. On Dec 4 the $PM_{2.5}$ and CO mass concentration increased a 29 and 40% compared to Dec 3 and the correlation got weaker with R^2=0.079.

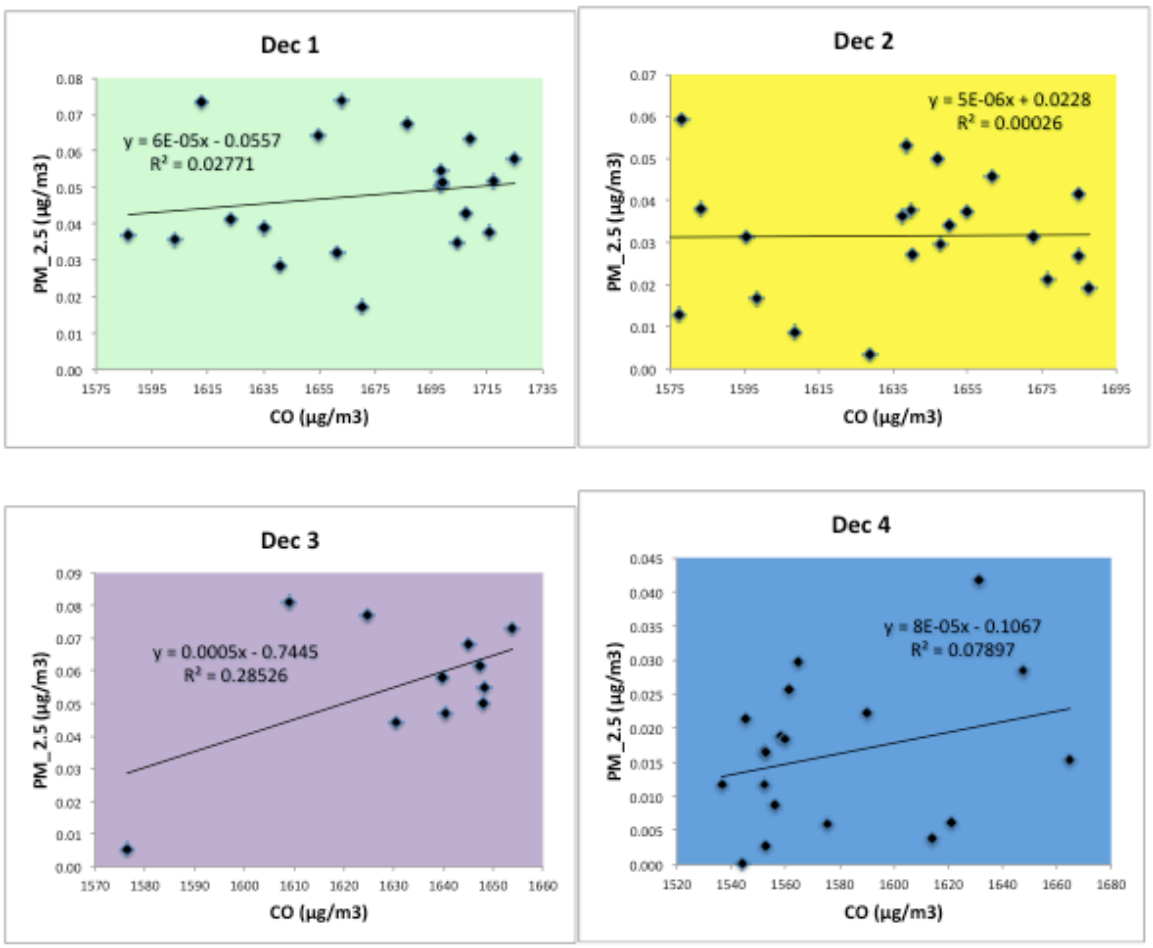

Figure 28. CO and $PM_{2.5}$ correlation for Dec 1-4

Dec 1 and 2 show the highest $PM_{2.5}$ mass concentration values of 0.62152 and 0.69548 µg/m^3, but the association between CO and $PM_{2.5}$ is imperceptible. This suggests that the presence of CO is bigger when the $PM_{2.5}$ is in lower concentration. Having small $PM_{2.5}$ concentration, the possibility for the CO to condensate over the particles is less and the CO could be found as a gas.

Figure 29 shows the SO_2 behavior related to $PM_{2.5}$ in which could be seen that the first two days the correlation was negative and very weak. However, during the two other days the association turned positive as denoted by the correlation coefficient of R^2=0.102 for Dec 3 and R^2=0.203 for Dec 4. These days the $PM_{2.5}$ mass concentration was lower than the two previous days.

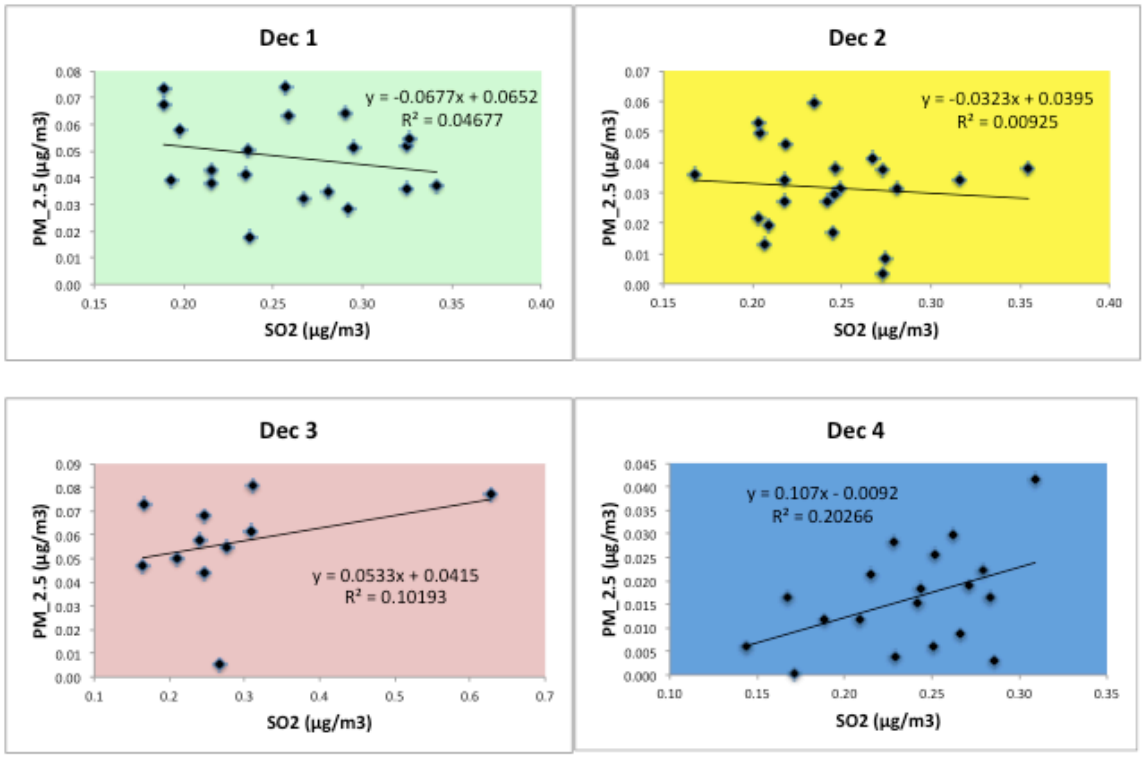

Figure 29. SO_2 and $PM_{2.5}$ correlation for Dec1-4

Figure 30 shows that O_3 had a variable association with $PM_{2.5}$ during these days. During Dec 3, the three trace gases were positively associated with $PM_{2.5}$ and the measured concentration for the gases and $PM_{2.5}$ was the lowest.

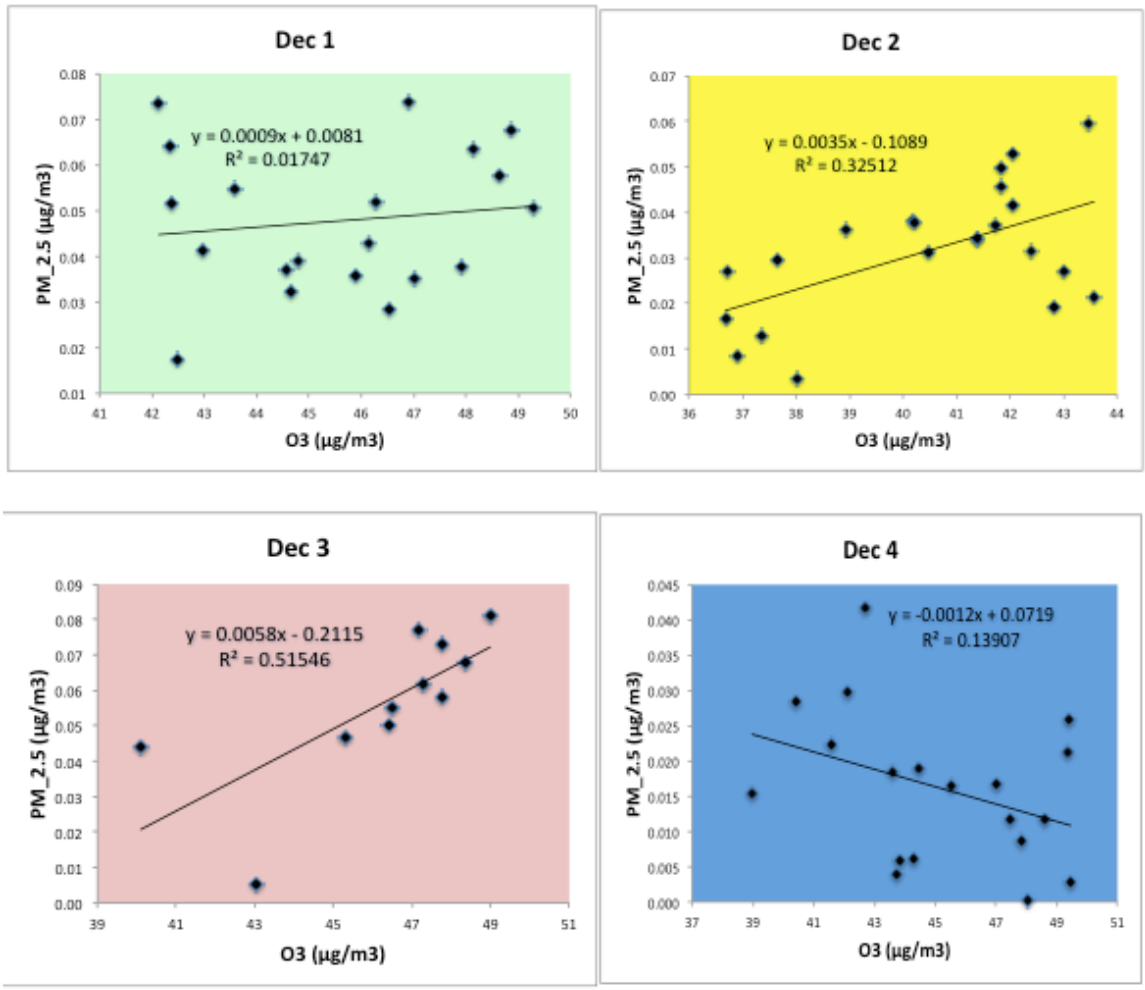

Figure 30. O_3 and PM2.5 correlation for Dec 1-4

Summary

The presence of CO, SO_2, and O_3, trace gases, and $PM_{2.5}$ that are well known as atmospheric pollutants was analyzed over the marine boundary layer of the tropical Atlantic Ocean. For Dec 1-4 the obtained mean aerosol mass concentrations were: 29320 ± 7953 µg/m³ for CO, 4.52± 1.04 µg/m³ for SO_2, 792± 190 µg/m³ for O_3 and 0.582 ± 0.12 µg/m³ for $PM_{2.5}$.

5. Conclusions

- A methodology was developed of using a cascade impactor and graphing the mass concentration per stage versus aerodynamic equivalent diameter. It has proven to be innovative and effective for characterizing particles of this nature.

- The established aerosol mass size distribution is unimodal with a maximum of 0.18794 $\mu g/m^3$ at 0.5 µm in the accumulation mode, which is characteristic of smoke particles. Hence, the shape of this distribution suggested that the air mass was composed of smoke particles, which was also confirmed by the models used. This result has the potential for both improving models and retrievals for space-based platforms (practical applications) as well as addressing fundamental science questions.

- Mass median aerodynamic diameter (MMAD) ranged from 0.57 to 0.72 µm and geometric standard deviation between 1.62 and 2.18 for accumulation mode, were calculated to evaluate the particle dimension composition during these four days.

- The mass concentration levels in the accumulation and coarse mode size ranges enabled the acquisition of quantitatively accurate modal information.
- The presence of CO, SO_2, and O_3, trace gases, and $PM_{2.5}$ that are well known as atmospheric pollutants was analyzed over the marine boundary layer of the tropical Atlantic Ocean. For Dec 1-4 the obtained mean aerosol mass concentrations were: 29320±7953 μg/m³ for CO, 4.52±1.04 μg/m³ for SO2, 792±190 μg/m³ for O3 and 0.582±0.12 μg/m³ for $PM_{2.5}$.
- The high CO concentration measured of 29320±7953 μg/m³ is a good example of how the African continent through fires contributes to release CO to the atmosphere.
- The significance of the measurements obtained is emphasized in light of the comparative scarcity of such data over the tropical Atlantic Ocean. The AEROSE data set is truly unique both with respect to the number of in-situ case studies but also the comprehensive measurement suite.

List of References

AEROSE. (2015). Retrieved from http://ncas.howard.edu/research-programs/aerose/

Airborne Particle. (1979). Baltimore: University Park Press.

Atia, A. A. (2010). *Observing aerosol mass densities during the trans-Atlantic transport of Saharan dust and biomass burning aerosols.* Retrieved from http://crest.ccny.cuny.edu/reu/mainframe/ckfinder/userfiles/files/Adam_Atia_Paper.pdf

Baron, P. A. (2011). *Aerosol measurement: principles, techniques, and applications.*

Berner, A. (1980). Mass size distributions of traffic aerosols at vVenna. *J. Phys. Chem. , 84*, 2079-2083.

Berner, A. (1996). Modal character of atmospheric black carbon size distributions. *Journal of Geophysical research , 101* (D14), 19,559-19,565.

California Measurements, Inc. (2002). *Air particles analyzer QCM cascade impactor.* Sierra Madre.

Calwater. (2015). Retrieved from http://www.esrl.noaa.gov/psd/calwater/overview/

Charlson, R. (1992). Climate forcing by anthropogenic aerosol. *Science , 225*, 423-430.

De Nevers, N. (2000). *Air pollution control engineering.* (M.-H. I. Editions, Ed.)

Draxler, R. a. (2003). *NOAA Air Resource Laboratory*. Retrieved from Hybrid single-Particle Lagrngian Integrated Trajectory Model: http:/www.arl.noaa.gov/ready/hysplit4.html

Duce, R. A. (1985). Sources, distributions, and fluxes of mineral aerosol and their relationship to climate, in Dalhem Workshop on Aerosol forcing of Climate. In R. L. Heintzenberg (Ed.). (pp. 43-72). John Wiley.

Estupinan, J. (2012, July). *Characteristics of the Saharan dust events observed in the month of July, 2012 at Miami, florida: Aerosol physical characteristics and vertical distribution.* Retrieved from www.srh.weather.gov/media/mfl/Dust_paper_July_2012.pdf

Gillette, D. A. (1977). Production of dust that maybe carried great distances, in desert dust: origin, characteristics, ad effect on man. (T. Pewe, Ed.) 11-24.

Ginoux, P. (2001). Sources and distributions of dust aerosol simulated with the GOCART Model. *J. Geophys. Res.* , 20,255-20,274.

Haywood, J. (2005). Can desert dust explain the outgoing longwave radiation anomaly over the Sahara during July 2003? *J. Geophys. Res.*

Hillamo, R. (2001). Modal structure of chemical mass size distribution in the high Artic aerosol. *Journal of Geophysical research , 106* (D21), 27,555-27,571.

Huang, J. (2010). African dust outbreaks: a satellite perspective of temporal and spatial variability over the tropical Atlantic Ocean. *Journal of Geophysical Research , 115*.

Intergovernmental Panel on climate change. (2007).

IPCC Fourth Assessment Report: Climate change 2007 (AR4). (2007). Retrieved from www.ipcc.ch/report/ar4

Jennings, S. (1991). Physical characteristics of ambient aerosols at Mace Head. *Atmos. Environ. , 25A*, 557-562.

Lau, K. (2007). Cooling of the Atlantic by Saharan dust. *Geophysical Research Letters , 34*.

Lewis, E. R. (2004). *Sea salt aerosol production: mechanism, methods, measurements and models: a critical review.* Washington, DC: American Geophysical Union.

Modis Web. (n.d.). Retrieved from modis.gsfc.nasa.gov/tools/

Moorthy, K. (2005). Aerosol characteristics and radiative impacts over the Arabian Sea during the intermonson season: results from ARMEX field campaign. *Journal of the Atmospheric Sciences , 62* (1), 192-206.

Morris, V. (2006, December 12). Measuring trans-Atlantic aerosol transport from Africa. *Eos* , 565-566.

Nair, V. S. (2008). Size segregated aerosol mass concentration measurements over the arabian Sea during ICARB. *Journal of Earth System Science , 117* (1), 315-323.

Nalli, N. (2011). Multi-year observations of the tropical Atlantic atmosphere: multidisciplinary applications of the NOAA AERosols and Ocean Science Expeditions (AEROSE). *Bulletin of the American Meteorological Society (BAMS) , 92* (6), 764-789.

Nalli, N. R. (2013). On the angular effect of residual clouds and aerosols in clear-sky infrared radiance observations 2. Satellite experimental analyses. *Journal of Geophysical Research: Atmospheres , 118*.

NASA's Goddard Space Flight Center. (2015, February 26). *NASA Visualization Explorer*. Retrieved May 3, 2015, from svs.gsfc.nasa.gov/cgi-bin/details.cgi?aid=11751

Prospero, J. M. (2002). Environmental characterization of global sources of atmospheric soil dust identied with the NIMBUS 7 total Ozone Mapping Spectrometer (TOMS) absorbing aerosol products. *Reviews of Geophysics , 40* (1).

Prospero, J. (1979). Mineral and sea salt aerosol concentration in various ocean regions. *J. Geophys. Res. , 84*, 725-731.

Pugatshova, A. (2007). Features of the multimodal aerosol size distribution depending on the air mass origin in the Baltic region. *Atmospheric Environment , 41*, 4408-4422.

Reddy, B. (2012). Ground-based in situ measurements of near-surface aerosol mass concentration over Anantapur: heterogeneity in source impacts. *advances in Atmospheric Sciences , 30* (1), 235-246.

Reid, J. (1994). Local Meteorological, transport, and source aerosol characteristics of late Autum Owens lake (dry) dust storms. *Atmospheric environment , 28*, 1699-1706.

Reist, P. C. (1984). *Introduction to aerosol science.* N.Y.: Macmillan publishing Company.

Roberts, G. (2009). Annual and diurnal African biomass burning temporal dynamics. *Biogeosciences , 6*, 849-866.

Roper, E. D. (In preparation). Surface-level ozone behaviour during Saharan dust outbreaks over the tropical Atlantic Ocean.

Sakerin, S. M. (2002). Spatial inhomogeneities and the spectral behaviour of atmospheric aerosol optical depth over the Atlantic Ocean. *J. Atmos. Sci. , 59*, 484-500.

Salam, A. (2008). Characteristics of atmospheric trace gases, particulate matter, and heavy metal pollution in Dhaka, Bangladesh. *Air Qual Atmos Health , 1*, 101-109.

Satellite-dust-6-16-1999.jpg. (1999, June 16). Retrieved from http:/health.usgs.gov/geohealth/images/satellite-dust-6-16-1999.jpg

Scheffer, F. a. (1992). *Lehrbuch Der Bodenkunde.* Frankfort, Germany.

Smirnov, A. (1995). Aerosol optical depth over the Oceans: analysis in terms of synoptic air mass types. *J. Geophys. Res. Atmos , 100* (D8), 16,639-16,650.

Tegen, I. (1996). The influence of climate forcing of mineral aerosols from distributed soils. *Nature , 380*, 419-422.

Todd, M. (2008, December). Quantifying uncertainty in estimates of mineral dust flux: an intercomparison of model performance over the Bodele depresion, Northern Chad. *Journal of Geophysical Research* .

TOMS dust and smoke (equatorial Africa). (1999, June 17). Retrieved from svs.gsfc.nasa.gov.

Twomey. (1977). The influence of pollution on the short-wave albedo of clouds. *J. Atmos. Sci. , 34*, 1149-1152.

Twomey, S. (1977). the influence of pollution on shorwave albedo of clouds. *J. Atmos. Sci. , 34*, 1149-1152.

Yaseen, S. (2014). Temporal variation of SO2 and NO2 concentration around Parichha thermal power plant, India. *Academic Journal , 6* (2), 6-12.

Curriculum Vita

Elsa Castillo earned her Master of Science degree in Physics from The University of Texas at El Paso (UTEP) in 2011. In August 2011, she joined the doctoral program in Environmental Science and Engineering at UTEP. Prior to attending the University of Texas, Dr. Castillo studied nuclear physics at Belarusian State University and gained experience in Cuba as a radiation physicist. She also worked, as a health physicist, on industrial radiation emission regulations and their enforcement for Dominican Republic Regulatory Agency.

Dr. Castillo was the recipient of numerous honors and awards including a University of Texas at El Paso College of Science Research Incentive Award and Spreading High-Performance computing Participation in undergraduate Education and Research (SHiPPER) Scholarship.

While pursuing her degree, Dr. Castillo worked as a research assistant for the Department of Physics and was member of the AERosol and Oceanic Scientific Expedition (AEROSE), participating in two expeditions over tropical Atlantic Ocean

in 2013. She interned at United Nations Committee on the Effects of Atomic Radiation (UNSCEAR), Vienna, Austria.

Dr. Castillo presented her research to the 2013 Pan American Advanced Studies Institute (PASI) on Atmospheric Processes in Latin America and the Caribbean: Observations, Analysis, and Impacts, Cartagena, Colombia and to the 2014 America Meteorological Society Annual Meeting.

Drs. Rosa Fitzgerald from UTEP and Vernon Morris from Howard University supervised Dr. Castillo's dissertation entitled, "Aerosol Physical and Chemical Properties Over the Tropical Atlantic Ocean,"

Recently Dr. Castillo was awarded the National Nuclear Security Administration Graduate Fellowship Program. This 12-months, full-time program allows her to work as a postdoctoral fellow at Livermore Field Office in global nuclear security and nonproliferation.